# REGULATION OF CALMODULIN GENE EXPRESSION IN THE RAT BRAIN STEM–MEDULLA REGION AFTER INDUCTION OF CHRONIC OROFACIAL SKIN INFLAMMATION AND SUBSEQUENT STEROID TREATMENT

Ivan Orojan, MD

Thesis supervisor: Karoly Gulya, PhD, DSc

Department of Cell Biology and Molecular Medicine
Faculty of Medicine and Faculty of Science and Informatics
University of Szeged
Szeged, Hungary

Szeged, 2008

*To my family*

**Publications directly related to the thesis:**

Bakota L., **Orojan I.**, Gulya K. (2005) Intranuclear differences in calmodulin gene expression in the trigeminal nuclei of the rat. *Acta Biol. Szeged.* 49, 9-14.

**Orojan I.**, Bakota L., Gulya K. (2006) Differential calmodulin gene expression in the nuclei of the rat midbrain-brain stem region. *Acta Histochemica* 108, 455-462.

**Orojan I.**, Szigeti C., Varszegi S., Gulya K. (2006) Dithranol abolishes UCH-L1 immunoreactivity in the nerve fibers of the rat orofacial skin. *Brain Research* 1121, 216-220.

**Orojan I.**, Bakota L., Szigeti C., Varszegi S., Gulya K. (2008) Experimentally induced orofacial inflammation and subsequent orticosteroid treatment differentially regulate calmodulin gene expression in the trigeminal nuclei of the rat. *Neurochem. Internat.* 52: 265-271.

**Presentations (talks, posters) directly related to the thesis:**

**Orojan I.**, Bakota, L., Szigeti C., Varszegi S., Gulya K. (2005) Orofacial skin inflammation upregulates calmodulin gene expression in the trigeminal nuclei of the rat. 3rd International Workshop for the Study of Itch, Heidelberg (poster No. 8) *Acta Derm Venereol* 85:477.

**Orojan I.**, Bakota, L., Gulya K. (2005) Experimentally induced orofacial skin inflammation upregulates calmodulin (CaM) gene expression in the medullar nuclei of the rat. 14th Congress of the European Academy of Dermatology & Venereology, London (abstract reference No. 805) . *J Eur Acad Dermatol Venereol*. 19(2) P04.67.

**Orojan I.**, Bakota L., Szigeti C., Varszegi S., Gulya K. (2005) Az orofaciális bőr gyulladása serkenti a calmodulin génexpressziót a patkány nyúltvelői magvaiban. *Bőrgyógyászati és Venerológiai Szemle* 81(6):*258/59*

**Orojan I.** (2006) Dithranol által kiváltott orofaciális gyulladás befolyásolja a calmodulin génexpressziót a patkány nyúltvelői magvaiban. *Magyar Bőrgyógyászok Nagygyűlése*, a Magyar Dermatológiai Társaság Fekete Zoltán Alapítványának nyertes előadása, Budapest.

**Table of contents**

**Abbreviations**

| | |
|---|---|
| $Ca^{2+}$ | calcium |
| $Ca^{2+}$/CaM kinase | $Ca^{2+}$-dependent/activated calmodulin kinase |
| CaM I, II, III | calmodulin genes I, II and III |
| CNS | central nervous system |
| cRNA | complementer ribonucleic acid |
| DIG | digoxigenin |
| dithranol | 1,8-dihydroxy-9(10H)-anthracenone (anthralin) |
| DNA | deoxyribonucleic acid |
| DTT | dithiothreitol |
| EDTA | ethylenediaminetetraacetic acid |
| Elocon$^{R}$ | mometasone furoate (9,21-dichloro-11,17-dihydroxy-16-methylpregna-1,4-diene-3,20-dione 17-(2-furoate)) |
| IgG | immunoglobulin G |
| mRNA | messenger ribonucleic acid |
| UCH-L1 | ubiquitin carboxyl-terminal hydrolase L1 |
| DIG | digoxigenin |
| Me5 | mesencephalic trigeminal nucleus |
| Mo5 | motor trigeminal nucleus |
| PBN | parabrachial nucleus |
| PBS | phosphate-buffered saline |
| PCR | polymerase chain reaction |
| Pr5 | principal sensory trigeminal nucleus |
| RT | room temperature |
| SDS | sodium dodecylsulfate |
| SDS/PAGE | sodium dodecylsulfate/polyacrylamide gel electrophoresis |
| Sp5 | spinal trigeminal nucleus |
| Sp5C | nucleus caudalis |
| Sp5I | nucleus interpolaris |
| Sp5O | nucleus spinal subnuclei oralis |
| SSC | sodium chloride, sodium citrate solution |
| SSPE | sodium chloride, sodium phosphate, EDTA solution |
| TBS | Tris-buffered saline |

| | |
|---|---|
| tRNA | transfer ribonucleic acid |
| UCH-L1 | ubiquitin carboxyl-terminal hydrolase L1 (PGP 9.5 gene product) |
| [$^{35}$S]UTP | $^{35}$S-labeled uridine triphosphate |

## 1. Summary

Dithranol (1,8-dihydroxy-9(10H)-anthracenone; anthralin) has been used to treat psoriasis for decades. Although its beneficial effect may involve the induction of cutaneous inflammation, and inflammation often leads to damage in nerve fibers in the periphery or, consequently, in the central nervous system (CNS) as well, these alterations, and especially those that elicit neuronal adaptation or regulation of neuronal gene expression, are not well documented. Accordingly, we investigated the effects of chronic dithranol treatment and subsequent corticosteroid treatment 1) on the immunohistochemical and Western blot characteristics of the cutaneous nerve fibers in the rat skin, where the epidermal nerve fiber component ubiquitin carboxyl-terminal hydrolase L1 (UCH-L1) was used as target antigene, and 2) on the regulation of calmodulin (CaM) gene expression on the different components of the rat trigeminal system in the midbrain–brain stem region; we used in situ hybridization techniques to detect gene-specific [$^{35}$S]- and digoxigenin (DIG)-labeled cRNA probes complementary to the multiple CaM mRNAs. The results of radioactive and color in situ hybridization histochemistries were analyzed with (semi)quantitative image-processing techniques.

Chronic dithranol treatment for 5 days resulted in a complete loss of UCH-L1 immunoreactivity. Topical application of corticosteroid onto the inflamed skin for 5 days reversed this effect: the UCH-L1 immunoreactivity was almost completely restored. Steroid treatment for 5 days did not change the appearance of the UCH-L1-immunoreactive nerve fibers. These findings were supported by Western blot analyses. We concluded that dithranol, incidentally similarly to psoriasis, causes inflammation and abolishes UCH-L1 immunoreactivity in the rat orofacial skin in a corticosteroid-reversible manner. This phenomenon may be due to the ability of dithranol to cause oxidative damage to UCH-L1 protein, and to the antioxidant activity of the corticosteroids countering this effect.

The different CaM genes were widely expressed throughout the midbrain–brain stem region with moderate intensities in the control animals. In spite of the similar general outline, significant differences in the distributions of the multiple CaM mRNA species were found in certain areas. In general, the CaM III mRNAs were most abundant, followed by the CaM I and CaM II mRNA populations. Most of the transcripts were found in the neuronal somata comprising the medullar nuclei, while much less label was detected in the neuropil. The CaM III mRNAs were more than 2.5 times more abundant than the CaM II mRNAs in the nucleus of the trapezoid body, and more than 2 times

more abundant in the motor trigeminal nucleus (Mo5), the principal sensory trigeminal nucleus (Pr5) and the olivary nucleus. The CaM III mRNAs were less dominant in the medial lemniscus, the inferior colliculus and the pontine reticular nucleus than those of the other CaM gene-specific transcripts. The CaM mRNA levels were low to moderate, without significant differences, in the mesencephalic trigeminal nucleus (Me5). The differential control of the expression of the CaM genes may therefore contribute to the regulation of the multiple neuronal functions linked to this complex brain region and regulated by different CaM-dependent mechanisms via its target proteins.

The quantitative analysis of the expression patterns of the three CaM genes revealed significant differences in the amounts of the transcripts of some CaM genes between the rostral and caudal parts of the individual nuclei of the trigeminal system in the control animals. In most cases, the CaM gene-specific transcripts displayed a clear differential distribution along the rostrocaudal axis: they were more abundant in the rostral parts of these nuclei. For example, the levels of mRNAs transcribed from each of the CaM I, II and III genes were significantly higher in the rostral part of the principal sensory trigeminal nucleus (Pr5), while the rostral part of the motor trigeminal nucleus (Mo5) exhibited an elevated amount of transcripts for the CaM I gene only. Interestingly, the CaM II mRNAs were most abundant in the caudal part of the Me5. Moreover, the largest difference between any of the CaM gene-specific transcript contents of the rostral and caudal parts was found for those of the CaM II gene in the Pr5. Here, the intranuclear difference was about 50%, the rostral part being the richer in CaM II mRNAs. Our results draw attention to the possible causal relation between the differences in the neuronal circuitry of the rostral and caudal parts of these nuclei and their differential CaM gene expression. This somatotopy may have important functional implications.

The cutaneous and mucosal surfaces in the infraorbital region around the whisker pad are innervated by the maxillary division of the afferent fibers of the trigeminal nerve, while certain ganglion cells project to the Pr5. In turn, some of the neurons in the Pr5 project to the Mo5, whose neurons do not innervate the infraorbital skin. We analyzed the CaM gene expression in these nuclei after dithranol-induced inflammation and subsequent treatment with corticosteroid in the infraorbital skin. CaM gene-specific mRNA populations were detected through quantitative image analysis of the distribution of CaM gene-specific riboprobes in brain stem cryostat sections of the control rats and of the rats chronically treated with dithranol, corticosteroid or both. These nuclei displayed a differentially altered CaM gene expression in response to the treatments. While the CaM

I and II mRNA contents were increased, the CaM III transcripts remained unaltered after chronic dithranol treatment in the Mo5. In the Pr5, however, the CaM mRNA contents were either unchanged (CaM I and III) or increased (CaM II). Subsequent corticosteroid treatment reversed the stimulatory effects of dithranol on the expression of all the CaM genes in the Mo5, but was without significant effects on the CaM I and II genes, or even increased the CaM III mRNA contents in the Pr5. Corticosteroid treatment alone was either ineffective or decreased the levels of CaM mRNAs in these nuclei. These data suggest that peripheral noxae of dermal origin may result in a trans-synaptically acting differential regulation of the multiple CaM genes in the brain.

## 2. Introduction

As a practising dermatologist, I have often mused about the possibility that dermatological disorders may have certain neurological consequences. Many skin diseases present both neurologic and dermatologic manifestations. Chronic itch is often seen by dermatologists. Pruritus and pain are aversive, but clearly distinct sensations originating in the peripheral nervous system and the CNS. Other disorders/anomalies of the skin are often classified as autonomic neurodermatological disorders (disorders of sweating and flushing, erythromelalgia, reflex sympathetic dystrophy, and livedo reticularis). During recent years, many interactions between itch and pain have been identified in acute transmission and sensitization processes. It is common experience that the itch sensation can be reduced by the painful sensations caused by scratching. Vice versa, analgesia may reduce this inhibition, and thus enhance itch. Classical inflammatory mediators such as bradykinin have been shown to sensitize nociceptors for both itch and pain. Regulation of gene expression induced by trophic factors, such as the nerve growth factor, plays important roles in persistently increased neuronal sensitivity for itch and pain. Thus, in light of the above, I was looked for a model (animal) system to study the neurological/neurobiological consequences of certain skin disorders.

Dithranol (anthralin) is one of the most widely used and effective, albeit empirical, topical treatments for patients with psoriasis (McBride et al., 2003; Swinkels et al., 2001; van de Kerkhof and Franssen, 2001; van der Vleuten et al., 1996). The molecular basis of its mode of action is still unknown, but it is probably related to the redox activity leading to the production of free radicals, including oxygen radicals (Lambelet et al., 1990; Shroot and Brown, 1986). A recent study (McGill et al., 2005) showed that dithranol accumulates in keratinocyte mitochondria, induces structural damage, and interferes with

the redox status of the endogenous ubiquinone pool at the level of the ubisemiquinone anion. These events lead to the increased generation of reactive oxygen species and eventually result in apoptosis.

There are some indications that either or both epidermal proliferation and/or keratinization and cutaneous inflammation may be crucial in the antipsoriatic effect of dithranol; indeed, the often serious inflammation and the irritative response of the perilesional or uninvolved skin are the most serious limitations to its use (Swinkels et al., 2002). Scratching human skin evokes an inflammatory reaction dependent in part on the sensory nerves (e.g. neurogenic inflammation; see Steinhoff et al., 2003 for references) in the dermis (McGrouther and Ahmad, 1998), while cutaneous inflammation following injury, surgical intervention, contact with chemical irritants, etc. affects the epidermal innervation. The extent of such inflammation on the peripheral nerves has been successfully demonstrated immunohistochemically by the use of the ubiquitin carboxyl-terminal hydrolase L1 (UCH-L1; gene aliases: pan-neuronal marker protein gene product (PGP) 9.5, ubiquitin thiolesterase, PARK5), a cytosolic deubiquitinating enzyme that is highly expressed both in humans and in animals (Doran et al., 1983). For example, the UCH-L1 immunoreactivity was decreased in the oral mucosa of patients with chronic inflammation caused by oral lichen planus (Nissalo et al., 2000), after the intradermal injection of capsaicin (Simone et al., 1998), in leprosy skin (Facer et al., 2000) and around the sweat glands in palmoplantar pustulosis (Hagforsen et al., 2000). The expression of UCH-L1 was absent in necrotic areas of the colon of rats treated with 2,4,6-trinitrobenzenesulfonic acid to induce experimental colitis (Poli et al., 2001), and its immunoreactivity was decreased in rats with nasosinusitis infected artificially with Staphylococcus bacteria (Ge et al., 2002). Interestingly, psoriasis, an inflammatory skin disorder often treated with dithranol, was reported to be accompanied by either decreased (Johansson et al., 1991) or unchanged (Al'Abadie et al., 1995) UCH-L1 immunoreactivity in the affected skin. In light of these conflicting results, we investigated whether the inflammation elicited by dithranol would affect the UCH-L1 immunoreactivity of the cutaneous nociceptive sensory fibers of the rat orofacial skin.

Deep and cutaneous orofacial tissue inflammation or painful temporomandibular disorders often elicit prolonged neuronal activation in the trigeminal nociceptive pathways that can lead to chronic pain, and they are therefore of paramount clinical importance. The neuroanatomical relationships between orofacial nociception and the trigeminal system are well documented (Waite and Tracey, 1995). The maxillary division

($V_2$) of the trigeminal ganglion innervates the cutaneous and mucosal surfaces of the infraorbital skin around the whisker pad, richly providing both deep and superficial nerves to the vibrissal follicles. The central processes of the neurons in the trigeminal ganglion are projected via the trigeminal root into the trigeminal tract and give collaterals to the principal sensory nucleus (Pr5) and, more caudally, to the spinal subnuclei oralis, interpolaris and caudalis (Waite and Tracey, 1995). Apart from the main projection of the Pr5 to the contralateral thalamus (Fukushima and Kerr, 1979), some of the neurons project to the motor trigeminal nucleus (Mo5; Travers and Norgren, 1983). The motor innervation of the infraorbital skin region is more complex, as it is provided independently by two motor nuclei. The motoneurons innervating the anterior and posterior segments of the deep masseter muscle are located in the Mo5, but other muscles (e.g. the buccinator and the orbicularis oculi) and the intrinsic muscles of the vibrissae, all situated in the infraorbital region, are innervated by neurons located in the facial nerve (Waite and Tracey, 1995).

A large number of data are available on the molecular, cellular and system-wide mechanisms involved in the development of, or the amelioration of pain related to, inflammation in the CNS. Nociceptive and pain-related information, mediated via different intracellular signalization processes, is transmitted and regulated at different levels of the CNS; from the point of view of our studies, the most important ones are those that shed light on the roles played by calmodulin (CaM) and its target proteins in the responses of the nervous tissue to the inflammatory stimuli.

CaM, a ubiquitous, multifunctional cytoplasmic calcium ($Ca^{2+}$) receptor protein encoded by three different genes in mammals, is especially abundant in the mammalian CNS (for recent reviews, see Palfi et al., 2002; Toutenhoofd and Strehler, 2000). Its regional distribution and expression pattern in the developing and adult rodent brain have been well documented by biochemical (Zhou et al., 1985), immunohistochemical (Caceres et al., 1983; Seto-Oshima et al., 1983, 1987) and in situ hybridization methods (Kortvely et al., 2002; Kovacs and Gulya, 2002, 2003; Ni et al., 1992; Palfi et al., 1999; Sola et al., 1996). Previous studies (some of them quantitative) at the Department of Cell Biology and Molecular Medicine (formerly the Department of Zoology and Cell Biology) have already documented the regional distribution and expression pattern of the multiple CaM genes during normal development and in adulthood in the rat brain. The expression patterns corresponding to the three CaM genes displayed a widely differential distribution for the CaM gene-specific mRNA populations throughout the brain and spinal cord

(Kortvely et al., 2002; Kovacs et al., 2002; Palfi et al., 1999, 2005). For example, we previously demonstrated a widespread and differential area-specific distribution of the CaM mRNAs in the developing (Kortvely et al., 2002) and adult rat CNS, under both physiological (Kovacs and Gulya, 2002, 2003; Palfi et al., 1999) and pathophysiological conditions (Palfi and Gulya, 1999; Palfi et al., 2001; Vizi et al., 2000). In the adult brain, the expression patterns corresponding to the three CaM genes differed most considerably in the olfactory bulb, the cerebral and cerebellar cortices, the diagonal band, the suprachiasmatic and medial habenular nuclei, and the hippocampus (Palfi et al., 1999). Moreover, the significantly higher CaM I and CaM III mRNA copy numbers than those of CaM II in the molecular layers of certain brain areas indicated a differential dendritic targeting of these mRNAs (Palfi et al., 1999); this notion was later demonstrated by immunocytochemical methods in primary hippocampal cultures (Kortvely et al., 2003) and by electron microscopic in situ hybridization techniques in the adult rat hippocampus (Palfi et al., 2005).

As CaM exerts its biological action through its target proteins that are involved in a number of cellular regulator processes (see Kennedy, 1989; Means et al., 1991; Palfi et al., 2002, for references), it is not surprising that immunohistochemical and in situ hybridization studies have demonstrated that CaM immunoreactivity or CaM gene-specific transcripts are often colocalized with those of the target enzymes of CaM within the same neuronal structures, not only in general, but in the brain stem–medulla region in particular (Erondu and Kennedy, 1985; Ichikawa et al., 2004; Ochiishi et al., 1998; Ogawa et al., 2005; Seto-Oshima et al., 1983; Strack et al., 1996). However, in spite of the number of neuronal functions associated with the midbrain–brain stem structures and regulated by CaM-dependent mechanisms (Bruggemann et al., 2000; Ogawa et al., 2005), there are only sporadic data on the distribution of CaM protein in this brain region (Seto-Oshima et al., 1983). Earlier light microscopic radioactive in situ hybridization studies from our own (Palfi et al., 1999) and another laboratory (Sola et al., 1996) did describe the distribution of the multiple CaM mRNA populations in the larger structures of the midbrain–brain stem areas of rats and mice, but the finer details are still unknown. In this respect, one of the unexplored areas concerns the trigeminal nuclei that form a complex sensory and motor system with precise somatotopic organization. The afferent components of this system carry various information from the skin of the face, the oral and nasal mucosa, and deeper structures such as subcutaneous tissues, facial muscles and tendons (Waite and Tracey, 1995). The head also contains several specialized structures

that receive trigeminal innervation, such as the teeth and tongue, the conjunctiva and cornea, and the vibrissae, which are under voluntary motor control (Dun, 1958). For rodents, the arrangement, the structure and the innervation of the facial vibrissae are similar (Rice et al., 1986), and the pattern is determined genetically (Van der Loos et al., 1984).

As mentioned above, in one of our previous studies (Palfi et al., 1999), we analyzed 16, mainly large structures in this area, where 5 of them exhibited significantly different CaM gene expressions. In order to gain more precise data for further functional studies, we have revisited and re-analyzed the quantitative distribution of the differential CaM gene expression in smaller areas of these structures, and also provided higher-resolution light microscopic images on the distribution of DIG-labeled CaM gene-specific cRNA probes.

Since CaM plays an important role in regulating a key target protein, $Ca^{2+}$-dependent/activated calmodulin kinase II ($Ca^{2+}$/CaM kinase II), in a number of neuronal functions related to the trigeminal system, including inflammation, neuropathic pain and nerve injury (Liu and Simon, 2003; Ogawa et al., 2005; Price et al., 2005), a precise, high-resolution mapping of the CaM gene expression could promote a deeper understanding of the functioning of the trigeminal system in health and disease. In this study, involving quantitative in situ hybridization analysis through the use of CaM gene-specific [$^{35}$S]-labeled cRNA probes, we also report on the differences in CaM gene expression patterns seen along the rostrocaudal axis within each nucleus of the trigeminal system.

Understanding the distribution of CaM-expressing cells in the normal, physiological situation helped us to detect and understand the changes in the regulation of CaM gene expression patterns after chronic peripheral skin, in this case orofacial, inflammation. We therefore set up experiments to map the changes in CaM gene expresion patterns associated with chronic dithranol and subsequent corticosteroid treatments in the trigeminal system of the adult rat.

**3. Specific aims**

Our objectives were to document the histological, immunohistological and Western blot characteristics of the inflamed orofacial skin after chronic dithranol treatment and corticosteroid reversal, and to localize and differentiate CaM mRNA populations transcribed from the multiple CaM genes in the different parts of the rat trigeminal

system after chronic inflammation of the infraorbital region of the orofacial skin by means of hybridization of transcript-specific riboprobes labeled with [$^{35}$S]UTP. Specifically, our aims were as follows:

1) To investigate the histochemical characteristics of the inflammation elicited by chronic dithranol treatment alone or in combination with corticosteroids, and of the UCH-L1 immunoreactivity of the cutaneous nociceptive sensory fibers of the rat orofacial skin after such treatment.
2) To localize, differentiate and semiquantitatively analyze in detail the different CaM mRNA populations transcribed from the multiple CaM genes in the adult normal rat midbrain–brain stem region,
3) and the possible rostrocaudal gradient by gene-specific [$^{35}$S]UTP- or DIG-labeled cRNA probes.
4) To localize and differentiate CaM mRNA populations transcribed from the multiple CaM genes in two prominent nuclei of the rat trigeminal system, namely the motor trigeminal (Mo5) and the principal sensory trigeminal (Pr5) nuclei, after chronic inflammation and reversal by corticosteroids of the infraorbital region of the orofacial skin by means of quantitative in situ hybridization.

## 4. Materials and Methods

### *4.1. Experimental animals*

The experimental procedures were carried out in strict compliance with the European Communities Council Directive (86/609/EEC), and followed the Hungarian legislation requirements (XXVIII/1998 and 243/1998) regarding the care and use of laboratory animals. Adult (200-220 g) male Sprague-Dawley rats were maintained under standard housing conditions and kept on a normal diet and tap water *ad libitum* with a 12-h light cycle (light on at 7.00 a.m.).

### *4.2. Chronic orofacial skin treatment*

The orofacial region (about 1 cm$^2$ around the whisker pad) on the right side of the animals was treated daily for 3 or 5 days, always in the morning, with a vaseline-based paste containing 10% dithranol (1,8-dihydroxy-9(10H)-anthracenone; Sigma, St. Louis, MO, USA). The control animals received either physiological saline or pure vaseline (petrolatum or vaselinum album; Sigma). Approximately 150 mg dithranol-containing

paste was applied on each occasion to the surface of the treated skin. After the fifth day of dithranol treatment, one group of animals were treated daily for 5 days with 0.1% corticosteroid lotion (Elocon$^{R}$; mometasone furoate, 9,21-dichloro-11,17-dihydroxy-16-methylpregna-1,4-diene-3,20-dione 17-(2-furoate); Schering, Kenilworth, NJ, USA). Approximately 400 mg mometasone fuorate lotion was applied on each occasion to the surface of the treated skin.

*4.3. Tissue preparation*

On the day following the last treatment, the rats were ether-anesthetized and decapitated between 1.00 and 3.00 p.m. The orofacial skin around the whisker pad and the brain stem–medulla area from the control and the treated animals were quickly removed, the brain stem–medulla area was separated, frozen and serially sectioned in a cryostat (20 μm) from bregma -8.80 mm to -9.30 mm (Paxinos and Watson, 1997) onto 3-aminopropyltriethoxysilane-coated glass slides and kept at -70 $^{o}$C until further processing, but not longer than 2 days.

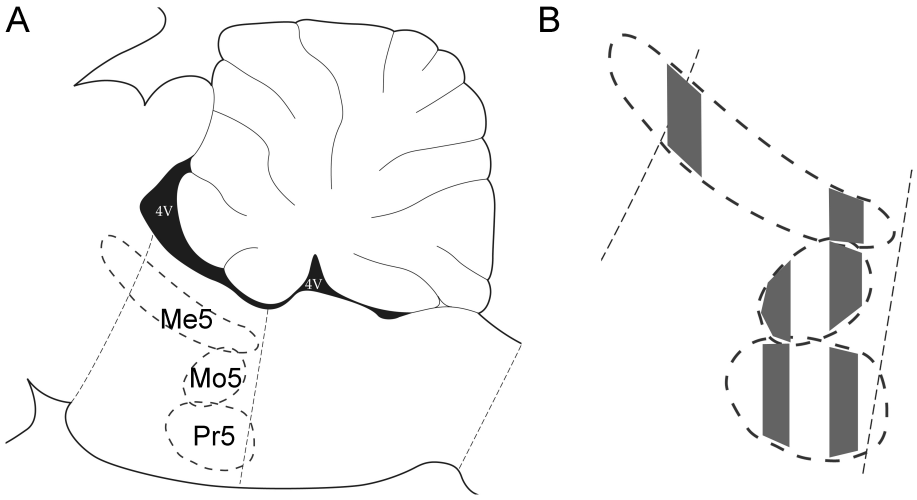


Figure 1. A) Schematic representation of the trigeminal nuclei (ovals outlined with dashed lines) in a section of the rat brain cut in a sagittal plane. Me5: mesencephalic trigeminal nuclei, Mo5: motor trigeminal nuclei, Pr5: principal sensory trigeminal nucleus, 4V: fourth ventricle. Note that these nuclei reside in different sagittal planes, and are never seen together as in this scheme (see also Fig. 9A, B). B) Enlarged schematic view of the trigeminal nuclei. The tissue sections (vertical areas shaded light gray) used for analysis in this study were cut from bregma -7.64 to -7.80 mm for the rostral, and -9.30 to -9.68 mm for the caudal part of Me5, from bregma -8.80 to -9.16 mm for the rostral, and -9.30 to -9.68 mm for the caudal part of Pr5, and from bregma -8.80 to -9.16 mm for the rostral, and -9.30 to -9.68 mm for the caudal part of Mo5 (coordinates according to Paxinos and Watson (1997)). The portion of Me5 that resides more rostral than indicated here is not suitable for the measurement of CaM gene expression because the cells cannot be grouped together with certainty.

The sections usually used in this study were cut from bregma -6.72 mm to -10.04 mm (Paxinos and Watson, 1997), encompassing the entire area where the trigeminal system (mesencephalic, motor and principal sensory trigeminal nuclei) resides (see Fig. 1 for details), but in certain cases, the midbrain–brain stem region was serially sectioned only from bregma -8.80 mm to -9.30 mm. In the rat, only the maxillary division of the trigeminal ganglion innervates the infraorbital region of the orofacial skin, the area of the treatment, supplying afferent fibers to cutaneous and mucous surfaces, while sensory inputs from this area are carried to the principal sensory and the different parts of the spinal trigeminal nucleus (Waite and Tracey, 1995). The spinal trigeminal nucleus was not included in this survey as its CaM gene expression pattern was weak, and did not allow an appropriate demarcation of this nucleus from other structures.

*4.4. Histology and immunohistochemistry*

Control and treated orofacial skin was quickly removed, serially sectioned in a cryostat (15 μm) onto 3-aminopropyltriethoxysilane-coated glass slides and kept at -70 $^{o}$C for 1-2 days until further processing. For histological assessment, cryostat sections of control and treated skin were stained in hematoxylin solution, dehydrated and covered with the synthetic resin DPX embedding medium (Sigma, St. Louis, MO, USA).

For UCH-L1 immunohistology, cryostat sections of skin samples were fixed in 4% formaldehyde in 0.05 M phosphate-buffered saline (PBS) for 5 min, treated against endogenous peroxidase activity with 1% $H_2O_2$ in 0.05 M PBS for 10 min at 37 $^{o}$C, and then incubated with a polyclonal rabbit antibody against human UCH-L1 (Chemicon, Temecula, CA, USA; 1:1,000) overnight at 4 $^{o}$C. The sections were then washed several times in 0.05 M PBS, and incubated with a biotinylated anti-rabbit IgG secondary antibody (Amersham Pharmacia Biotech, Buckinghamshire, England; 1:200) for 6 h at room temperature (RT). After several washes in 0.05 M PBS, the sections were finally incubated with a biotinylated streptavidin peroxidase tertiary antibody (Amersham; 1:200) overnight at 4 $^{o}$C. Immunoreactivity was visualized for 10 min by using 0.5 mg/ml diaminobenzidine in 0.01% $H_2O_2$. The sections were washed as before, dehydrated, and covered with DPX.

*4.5. Western blot analysis*

For Western blotting, rats were perfused transcardially with ice-cold PBS solution. Control and treated orofacial skin samples were cut (about 1 $cm^2$), minced with scissors

and homogenized in 50 mM Tris-HCl (pH 7.5) containing 150 mM NaCl, 0.1% Nonidet P40, 0.1% cholic acid, 2 μg/ml leupeptin, 1 μg/ml pepstatin, 2 mM phenylmethylsulfonyl fluoride and 2 mM EDTA, centrifuged at 15,000 g for 10 min. The pellet was discarded and protein concentrations were determined on the supernatant according to the method of Lowry et al. (1951). Fifty μg protein was separated on a 12% SDS-polyacrylamide gel and transferred onto Hybond-ECL nitrocellulose membrane (Amersham Biosciences, Little Chalfont, Buckinghamshire, England), blocked for 1 h in 5% nonfat dry milk in Tris-buffered saline (TBS) containing 0.1% Tween 20, and incubated for 1 h with the UCH-L1 polyclonal antibody (1:2,000). After five washes in 0.1% TBS-Tween 20, the membranes were incubated for 1 h with a peroxidase-conjugated goat anti-rabbit antibody (Jackson ImmunoResearch Europe Ltd. Cambridgeshire, United Kingdom; 1:4,000), and washed five times as before. The enhanced chemiluminescence method (ECL Plus Western blotting detection reagents; Amersham Biosciences) was used to reveal immunoreactive bands according to the manufacturer's protocol.

*4.6. Generation of CaM gene-specific cRNA probes*

Briefly, genomic sequences of the 3'-nonhomolog regions of the CaM I, II and III mRNAs were amplified by polymerase chain reactions (PCRs) as described previously (Palfi et al., 1998); sequence alignment was completed with the software BLASTN version 2.0.6 (Zhang and Madden, 1997). PCRs were performed by employing EcoR I and BamH I restriction enzyme cleavage site-extended primers. The primer sequences complementary to rat genomic DNA were as follows: for CaM I, 5'-AGACCTACTTTCAACTACT, corresponding to the 30-48-bp sequence, and 5'-TGTAAAACTCATGTAGGGG, corresponding to the 236-254-bp sequence of exon 6 (Nojima and Sokabe 1987); for CaM II, 5'-ATTAGGACTCCATTCCTCC, corresponding to the 144-162-bp sequence (numbered 1929-1947), and 5'-CACAACTCCACACTTCAACAGC, corresponding to the 353-374-bp sequence (numbered 2138-2159) of exon 5 (Nojima 1989); and for CaM III, 5'-ATGATGACTGCGAAGTGAAG, corresponding to the 12-31-bp sequence (numbered 7058-7077) of exon 6, and 5'-CAGGAGGAAGGAGAAAGAGC, corresponding to the non-transcribed genomic sequence 153-172-bp downstream to the stop codon (numbered 7228-7247; Nojima 1989). Standard PCRs were run for 35 cycles (Palfi et al. 1998), and the resulting PCR products were cloned into a pcDNA3 vector (Invitrogen Corp.,

Carlsbad, CA, USA) and sequenced (AB 373 DNA Sequencer, PE Applied Biosystems, Foster City, CA, USA) to confirm their identity. In vitro RNA syntheses from the purified and linearized vectors were carried out to prepare antisense and sense cRNA probes. The complementary probe sequences were 225 bp (CaM I), 231 bp (CaM II) and 157 bp (CaM III) long. For radiolabeling, [$^{35}$S]-UTPαS (1100 mCi/nmol; Isotope Institute, Budapest, Hungary) was incorporated, using Riboprobe System-T7 and Riboprobe System-SP6 (Promega; Madison, WI, USA) according to the manufacturer's instructions. Labeled probes were purified by size exclusion chromatography. The probe-specific activities of the radiolabeled hybridizing sequences were determined to be 1.97-4.38 x $10^7$ cpm/pmol. The specificity of the 3 antisense probes had previously been determined by sequence alignment, Northern blot analysis and in situ hybridization (Palfi et al., 1998, 1999).

*4.7. Radioactive and color in situ hybridization*

The protocol for radioactive in situ hybridization with [$^{35}$S]-labeled CaM gene-specific cRNA probes was carried out according to Palfi et al. (1998, 1999). Briefly, coronal cryostat sections from the brain stem–medulla region were fixed for 5 min in 2x SSC containing 4% formaldehyde, washed twice in 2x SSC for 1 min, and then rinsed in 0.1 M triethanolamine containing 0.25% acetic anhydride at RT for 5 min. The sections were dehydrated and hybridized in 100 μl hybridization solution (50% formamide, 5x SSPE, 1x Denhardt's reagent, 10% dextran sulfate, 50 mM DTT, 100 μg/ml salmon sperm DNA and 100 μg/ml yeast tRNA) containing 200 fmol/ml [$^{35}$S]- or 200 ng/ml DIG-labeled riboprobe. The pH of the solution was adjusted to 7.4. Hybridization was performed under parafilm coverslips in a humidified chamber at 45 °C for 20 h. The sections hybridized with [$^{35}$S]-labeled riboprobes were extensively rinsed in 2x SSC/50% formamide at 50 °C, treated with 16 μg/ml RNase A at 37 °C for 30 min, washed again in 2x SSC/50% formamide at 50 °C, and then dehydrated, air-dried and processed for autoradiography.

The color in situ hybridization procedure was based on our previously described protocols for DIG-labeled CaM gene-specific riboprobes (Kovacs and Gulya, 2002, 2003). The sections were hybridized with DIG-labeled riboprobes in 100 μl hybridization solution at 55 °C for 20 h. After hybridization, the sections were washed first in buffer B1 (100 mM Tris-HCl pH 7.5, 150 mM NaCl) at RT for 5 min, then in 2x SSC/50%

formamide at 55 °C for 5 min, and rinsed again several times in 2x SSC at RT. The sections were then blocked in 5% heat-inactivated sheep serum in B1 at RT for 2 h and incubated in sheep anti-DIG-alkaline phosphatase conjugate (Boehringer Mannheim GmbH, Mannheim, Germany; 1:1000 dilution) in 5% sheep serum in B1 at 4 °C for 24 h. Sections were washed in B1 for 3 x 5 min, and then in buffer B2 (100 mM Tris-HCl pH 9.5, 100 mM NaCl, 50 mM $MgCl_2$) for 10 min, and were developed in B2 containing 340 μg/ml nitro blue tetrazolium and 180 μg/ml 5-bromo-4-chloro-3-indolyl phosphate for 24 h under darkroom conditions. The color reaction was terminated by rinsing the sections in 10 mM Tris-HCl (pH 8.0), 1 mM EDTA for 5 min at RT. The sections were then dehydrated and covered with glycerol.

*4.8. Autoradiography and image analysis*

Tissue sections hybridized with radioactive riboprobes were exposed to Kodak BioMax MR-1 films (Eastman Kodak Co., Rochester, NY, USA) for 5 days at -20 °C and developed. At least three separate hybridization experiments for each animal were carried out for each CaM gene, and the gray-scale values for each CaM gene were measured in at least four consecutive sections. Autoradiographic images of hybridized sections were scanned at 600 x 600 dpi resolution and and analyzed by the computer program Image J (version 1.32; developed at the U.S. National Institutes of Health by W. Rasband, and available from the Internet at http://rsb.info.nih.gov/ij). Regions of interests were outlined on the computer screen and their signal intensities were measured. Gray values between 0 (lightest) and 255 (darkest) were assigned to the grayness of the images, and the specific gray values were determined by subtracting the sense values from the corresponding antisense values. Some of the sections were counterstained with toluidine blue or safranin to define the structural organization of the brain stem–medulla area. It is important to note that some parts of the brain stem–medulla area were not included in this survey as their CaM gene expression patterns were so weak that they did not allow an appropriate demarcation of certain nuclei from other structures, or certain areas, such as the dorsolateral and ventromedial parts of the Mo5, could not be delineated properly on the basis of the autoradiographic distribution of their CaM gene-specific mRNA contents. For example, we were unable to discriminate between certain parts of the Pr5; accordingly, gray-scale values for its dorsomedial and ventrolateral parts are not reported separately here.

For color in situ hybridization, hybridized medullar sections were examined under a Leica DM LB microscope (Leica Mikroskopie und Systeme GmbH; Wetzlar, Germany). Microscopic images (1600 x 1200 pixels, 8-bit gray scale) were captured with a Canon EOS 300D digital camera (Canon Inc., Tokyo, Japan) connected to a Power Macintosh G5 computer.

*4.9. Statistics*

Analysis of significance was carried out with the two-tailed Student's *t*-test (Microsoft Excel 2004 for Mac, Ver. 11.2; Microsoft, Redmond, WA, USA). For Western blots, values were presented as means ± S.D. from three blots of three independent experiments. For the gene expression studies, at least 3 separate hybridization experiments for each animal were carried out for each CaM gene, and the gray-scale values for each CaM gene were measured in at least 4 consecutive sections. These values were represented as means ± S.D.

## 5. Results

*5.1. Effects of dithranol and corticosteroid on orofacial skin inflammation and UCH-L1 immunoreactivity*

The animals treated with dithranol began to rub their perioral area, predominantly with their ipsilateral paw, within 1 h and continued to do so throughout the entire treatment regimen. Reddened perioral swelling was evident on the treated surface after about 3 h. Rats receiving physiological saline did not exhibit paw-related behavioral reactions or perioral inflammation. The alterations in the appearance of the rat orofacial skin as consequences of the treatments are seen in Fig. 2.

Dithranol treatment resulted in severe inflammation in the orofacial skin, as evidenced by hematoxylin staining and UCH-L1 immunohistochemistry. The histological signs of the inflammation were already evident after 3 days of treatment (data not shown), but were more severe after 5 days of dithranol treatment; by this time, some hair loss also occurred. In the inflamed tissue, hematoxylin staining demonstrated the usual histological signs of severe skin inflammation, e.g. hyperkeratinization, abnormal thickening of the stratum corneum, and acanthosis (Fig 3B). Corticosteroid treatment reversed these symptoms in the diseased animals (Fig 3C).

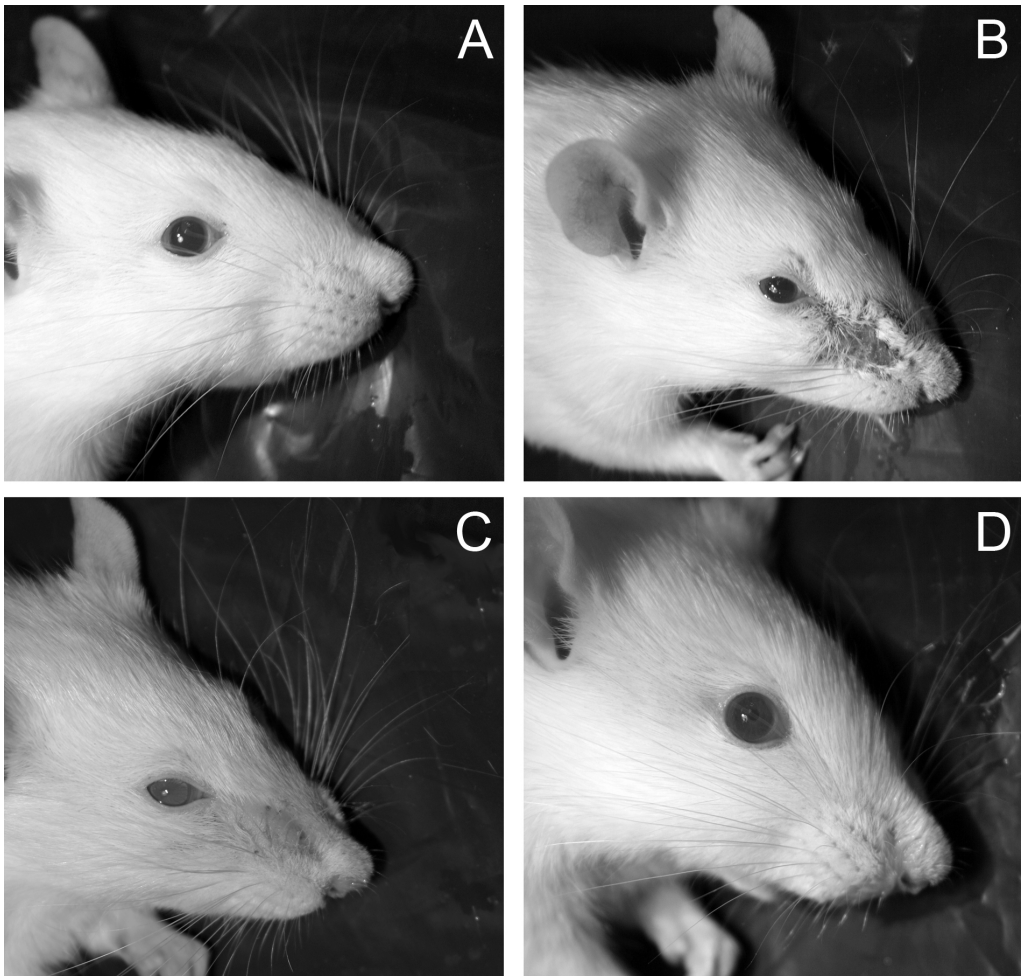


Figure 2. Effect of chronic inflammation and its treatment on the appearance of the rat orofacial skin. A) control, B) dithranol-treated for 5 days, C) dithranol-treated for 5 days, then treated with steroid for 5 days, D) steroid-treated for 5 days.

As revealed by hematoxylin staining, corticosteroid treatment alone did not have any histological effect (Fig. 3D). When UCH-L1 was visualized, heavy immunoreactivity was seen in the perifollicular fibers in the normal skin (Fig. 3E), whereas the dithranol-treated inflamed skin was characterized by a complete loss of these fibers (Fig. 3F). Topical corticosteroid treatment of the inflamed skin for 5 days almost completely restored the UCH-L1 immunoreactivity in the cutaneous sensory nerves (Fig. 3G), while the same steroid treatment alone did not have any effect on the UCH-L1 immunoreactivity of the neuronal elements of the orofacial skin (Fig. 3H). These immunohistochemical findings were supported by Western blot analysis. An UCH-L1-immunoreactive band of the expected size (approx. 27 kDa) was detected from control and treated tissues (Fig. 4). The intensities of the bands were similar for the control, corticosteroid-treated and dithranol- and steroid-treated samples, while the average intensity of the dithranol-treated samples was only 39.5% of the control value.

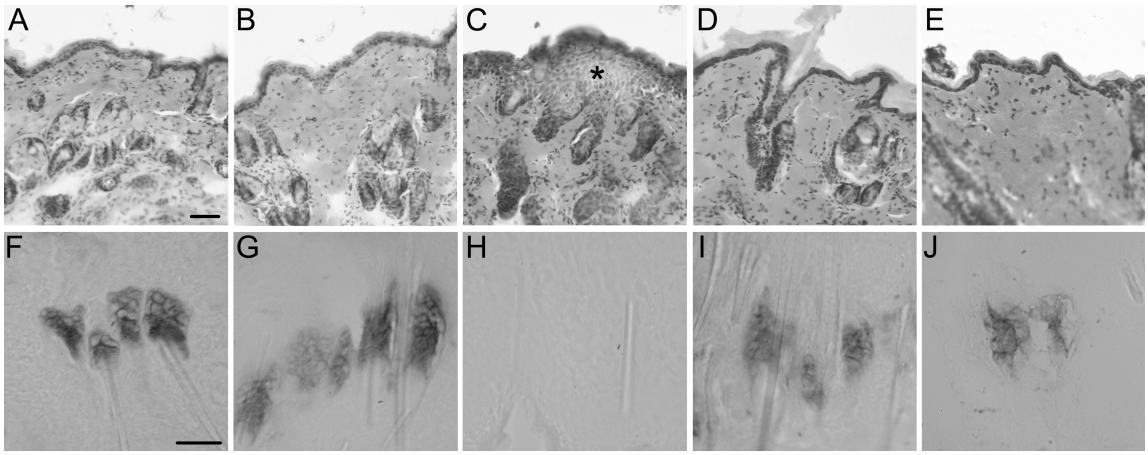


Figure 3. Histological features and UCH-L1 immunoreactivity of control and treated rat skin. A-E: hematoxylin staining, F-J: UCH-L1 immunoreactivity. A, F: control orofacial skin treated with physiological saline. B, G: control orofacial skin treated with pure vaseline. C, H: skin inflammation after dithranol treatment for 5 days. D, I: amelioration by steroid treatment for 5 days of skin inflammation elicited by dithranol treatment for 5 days. E, J: 5-day steroid treatment alone. No differences in histological features or UCH-L1 immunoreactivity are observed between the physiological saline- and vaseline-treated control skin samples (see A *vs* B and F *vs* G). Signs of severe skin inflammation, e.g. hyperkeratinization, abnormal thickening of the stratum corneum, and acanthosis (asterisk) are evident in hematoxylin-stained sections (B). After corticosteroid treatment, the skin regains its normal histological appearance, although some indications of mild hyperkeratinization still exist (C). Corticosteroid treatment alone did not change the normal structure of the orofacial skin (D). Heavy UCH-L1 immunoreactivity can be seen in the perifollicular fibers in the normal skin (E), whereas the inflamed skin is characterized by the complete absence of these fibers (F). Corticosteroid treatment of the inflamed skin for 5 days strongly favored reappearance of the UCH-L1 immunoreactivity (G). Steroid treatment alone did not affect the UCH-L1 immunoreactivity of the neuronal fibers of the orofacial skin (H). Scale bars: 50 μm (A-G).

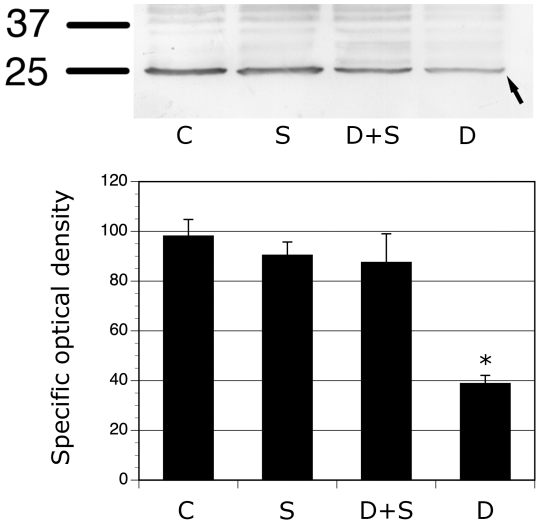


Figure 4. Comparison of the UCH-L1 protein levels in orofacial skin samples by Western blot analysis. Aliquots of the homogenized orofacial skin samples were subjected to SDS/PAGE (12% gel) and electrophoretically transferred to nitrocellulose membrane; blots were assayed for reactivity toward a polyclonal rabbit antibody directed against human UCH-L1 (Chemicon). A strong immunopositive band at around 24 kDa (arrowhead) was detected in the control and the treated orofacial skin samples. Much lighter bands with larger molecular weights can be seen in the gel. The positions of the markers (25 and 37 kDa) are indicated. Specific optical density values (after subtraction of the background values) were calculated as means ± S.D. from 3 separate experiments (*$p < 0.05$, Student's *t*-test). C (control skin sample treated with physiological saline):

98.08 ± 6.70 (100%); S (steroid treatment): 90.37 ± 5.35 (92.1% of the control value); D+S (dithranol treatment followed by steroid treatment): 87.45 ± 11.54 (89.2% of the control value); D (dithranol treatment): 38.79 ± 3.30 (39.5% of the control value).

*5.2. CaM gene expression in the midbrain–brain stem region*

The structures of the midbrain–brain stem region that are distinguishable on autoradiographic films within the range from bregma -8.80 mm to -9.30 mm and that were used for quantitative measurements of CaM gene-specific mRNA populations are depicted in Fig. 5. These nuclei are either completely encapsulated in this block of tissue or a sizeable portion of their masses lies within this range.

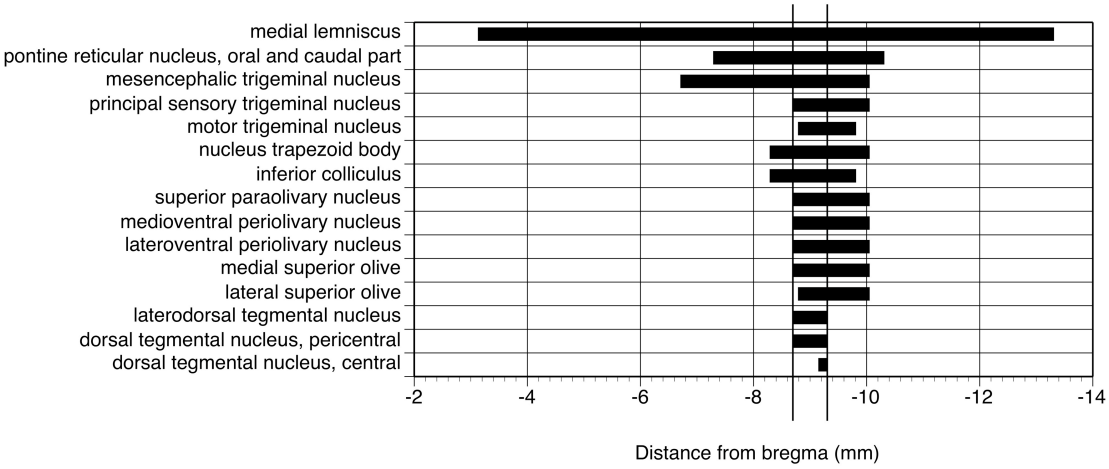


Figure 5. Diagrammatic representation in the sagittal plane of the nuclei of the brain stem–medulla in the rat brain. Distances from the bregma (rostral and caudal ends) for each nucleus are indicated in mm as reported by Paxinos and Watson (1997). Vertical lines (at bregma -8.80 mm and -9.30 mm) indicate the tissue block from which the cryostat sections were cut for in situ hybridization. The nomenclature of the neuronal structures used is that of Paxinos and Watson (1997).

In situ hybridization of radioactive antisense CaM I, II and III cRNA probes to tissue sections of the medulla established a specific and unique distribution (Fig. 6A-C), whereas hybridization with a sense probe resulted in very low labeling with nonspecific distribution (Fig. 6D). CaM gene-specific mRNAs transcribed from the three CaM genes were widely distributed throughout the midbrain–brain stem region. In general, a differential distribution and a medium quantity of CaM gene expression were demonstrated mainly in the nuclei of the brain stem–medulla enriched in neuronal cell bodies, in contrast with the more even, but lower, hybridization signals of the surrounding neuropil.

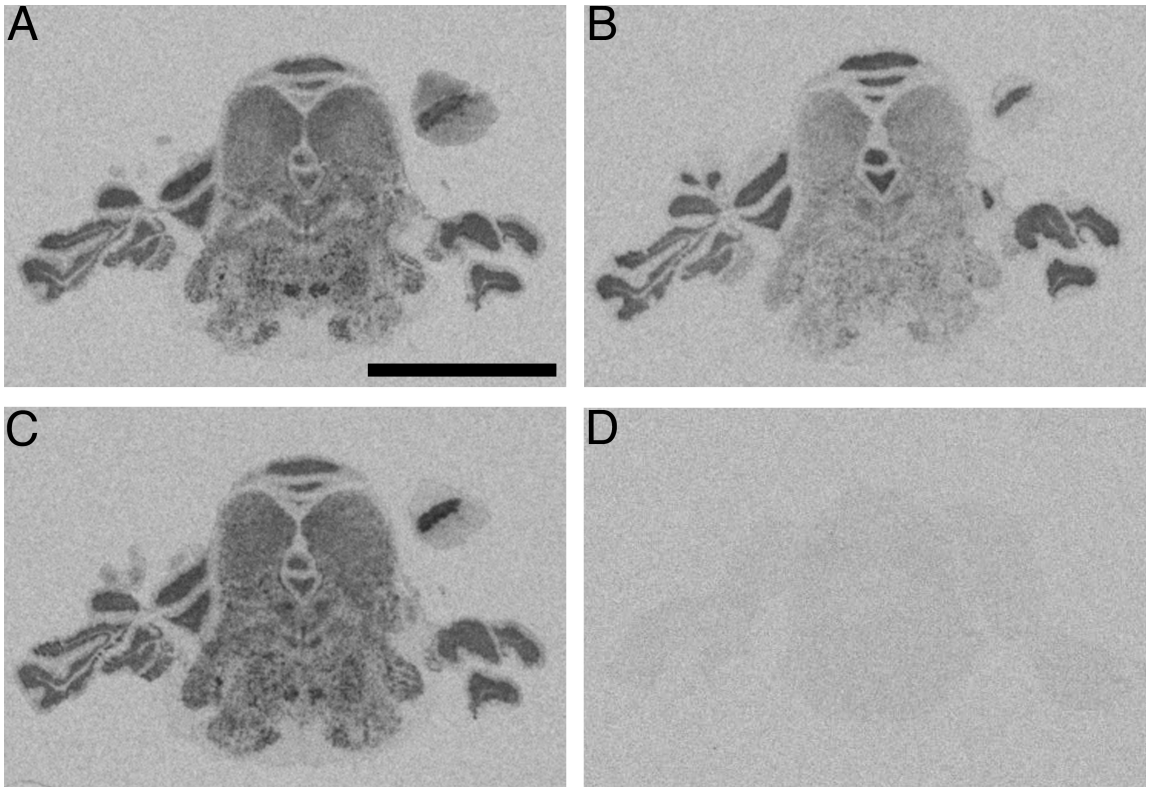


Figure 6. Differential CaM gene expression in the medullar nuclei of the rat brain. In situ hybridization of antisense probes to the tissue sections established a specific and unique distribution for CaM I (A), CaM II (B) and CaM III (C) mRNA populations, while hybridization with sense probes resulted in very low labeling with nonspecific distribution (D). The portions of the cerebellum seen in these pictures where the CaM gene expression is much more balanced clearly demonstrate the low representation of CaM II mRNAs in the medulla. Representative pictures taken at approximately bregma -9.16 mm (Paxinos and Watson, 1997). Scale bar: 0.5 cm.

In most of the neuronal structures analyzed, the mRNAs transcribed from the CaM III gene were most abundant, followed in sequence by the CaM I and CaM II mRNA populations (Table 1). Specifically, the rank order of abundance in the nuclei of the midbrain–brain stem region investigated was CaM III > CaM I > CaM II, except in the medial lemniscus, where it was CaM I ≈ CaM III > CaM II, and in the Me5, where the CaM mRNA levels were moderate, and the different CaM mRNA populations were present in practically equal proportions, without significant differences. The largest differences in the multiple CaM mRNA populations exceeded 2-fold. For example, the CaM III mRNAs were 2.43 and 2.53 times more abundant than the CaM II mRNAs in the Pr5 or in the trapezoid body, respectively, and more than 2 times as abundanat in the Mo5.

**Table 1.**

| Brain area | Specific gray-scale values | | |
|---|---|---|---|
| | CaM I | CaM II | CaM III |
| Mesencephalic trigeminal nucleu | 65.64±7.37 | 67.59±11.23 | 73.11±17.96 |
| Motor trigeminal nucleus | 71.87±11.38* | 40.81±6.46** | 82.74±9.07 |
| Principal sensory trigeminal nucleus | 77.29±5.24* | 33.9±8.32** | 82.42±3.89 |
| Tegmental nucleus | 69.07±7.58* | 54.1±5.41** | 82.25±7.05 |
| Trapezoid body, nucleus | 47.28±20.36 | 32.22±11.45** | 81.5±12.29*** |
| Medial lemniscus | 88.11±12.63 | 64.35±7.16** | 86.65±7.98 |
| Inferior colliculus | 64.87±4.51* | 46.25±8.73** | 71.67±5.13 |
| Pontine reticular nucleus | 69.33±5.00* | 34.82±9.18** | 72.91±6.1 |
| Olivary nucleus | 49.4±9.4* | 26.59±5.11** | 61.94±8.92 |

Quantitative analysis of CaM gene expression in the adult rat medulla. Coronal cryostat sections from the medulla were cut, hybridized separately with antisense [$^{35}$S]cRNA probes specific for CaM I, CaM II, or CaM III mRNAs and exposed to autoradiographic film. Film autoradiographic images (at least 4 for a given structure in each of the 5 animals) were analyzed by computer-assisted microdensitometry. Gray-scale levels for each CaM gene in all retinal layers were determined by using the image analysis computer program Image J v1.32. High-resolution gray-scale images were taken and the medullar structures of interest were outlined on the computer screen. Specific gray-scale values (means of at least 20 measurements from 5 separate experiments ± S.D.) were calculated by subtracting the nonspecific values resulting from the hybridization of the respective sense cRNA probes from those of the values of the antisense [$^{35}$S]cRNA probes. The tegmental nucleus encompasses the following regions: the pericentral part of the dorsal tegmental nucleus, the central part of the dorsal tegmental nucleus and the laterodorsal tegmental nucleus. The olivary nucleus consists of the following regions: the lateral superior olive, the lateroventral periolivary nucleus, the medioventral periolivary nucleus, the superior paraolivary nucleus, and the medial superior olive. Significant differences ($p < 0.01$, two-tailed Student's *t*-test) were found between the CaM I and CaM II (*), CaM II and CaM III (**) and CaM I and CaM III genes (***).

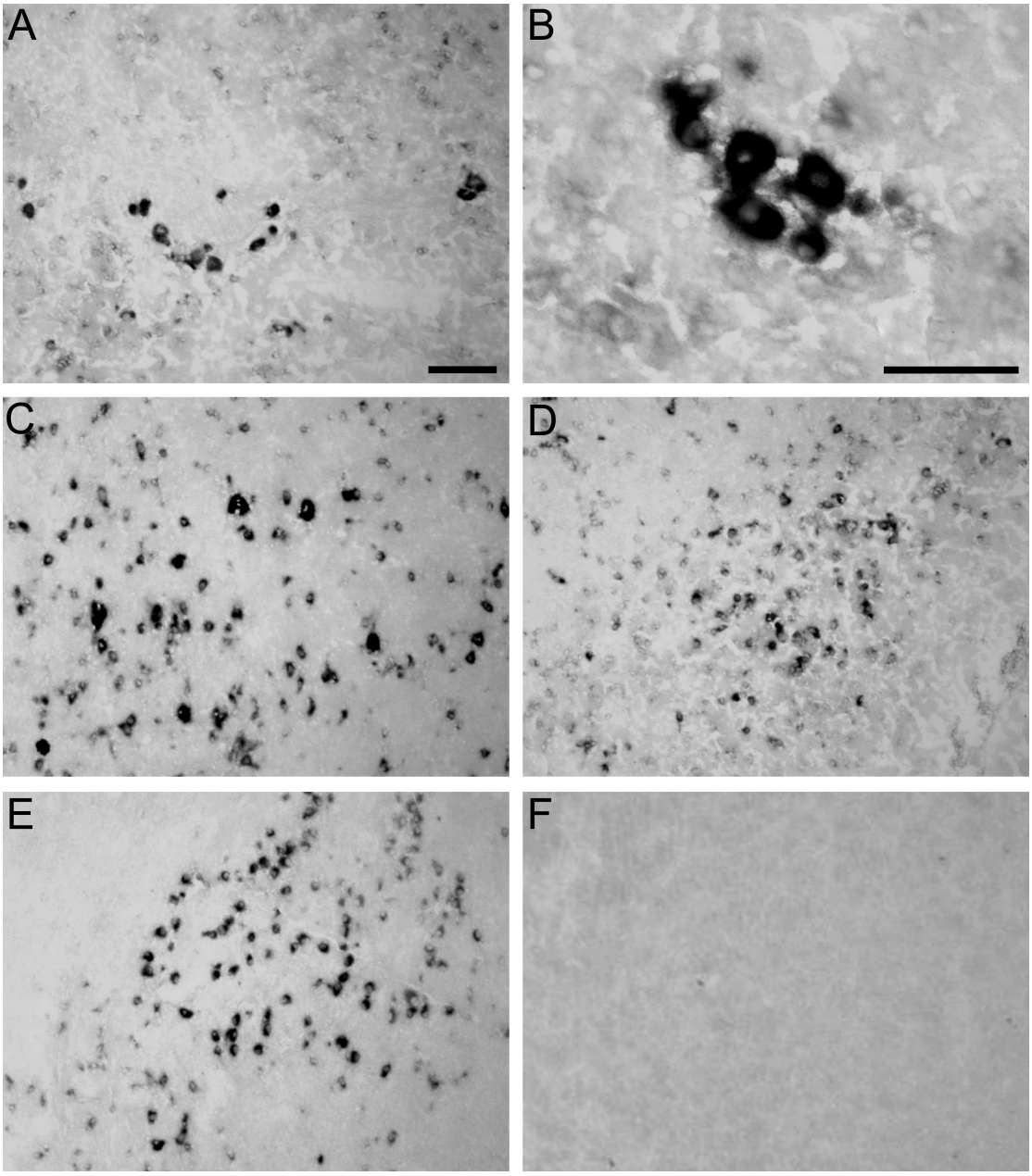

Figure 7. Representative in situ hybridization pictures of DIG-labeled CaM I-specific riboprobes in selected medullar nuclei. A, B: mesencephalic trigeminal nucleus, C: motor trigeminal nucleus, D: tegmental nucleus, E: trapezoid body, F: in situ hybridization with a sense probe. Scale bars: 50 μm (A, C-F), 25 μm and 100 μm (B).

In spite of the similar rank order of CaM mRNA abundances, however, significant differences in the distributions of the multiple CaM mRNA species were found for certain areas of the midbrain–brain stem region when DIG-labeled CaM I gene-specific cRNA probes were used. Color in situ hybridization demonstrated many, primarily medium-sized multipolar neurons in the medullar nuclei (Figs 7 and 8). The neuropil was usually low in CaM I mRNAs (Figs 7A-E and 8A-F). Most of the intraneuronal precipitate was perinuclear, leaving the nucleus visible by its lighter label, with occasional labeling seen

in the proximal parts of the main dendrites (Fig. 7B). The expressions of the three CaM genes were at lower levels in the small interneurons (see Fig. 7C, E for representative pictures on the CaM I mRNA distribution in these cells). Neuronal somata for transcripts for one CaM gene or other were strongly labeled in all nuclei investigated. A large number of small neurons with uniformly strong labeling were found to express CaM I mRNAs in the Mo5 (Fig. 7C), while neurons with similar sizes but with different label intensities for the CaM I gene were characteristic for the tegmental nucleus (Fig. 7D) and the trapezoid body (Fig. 7E).

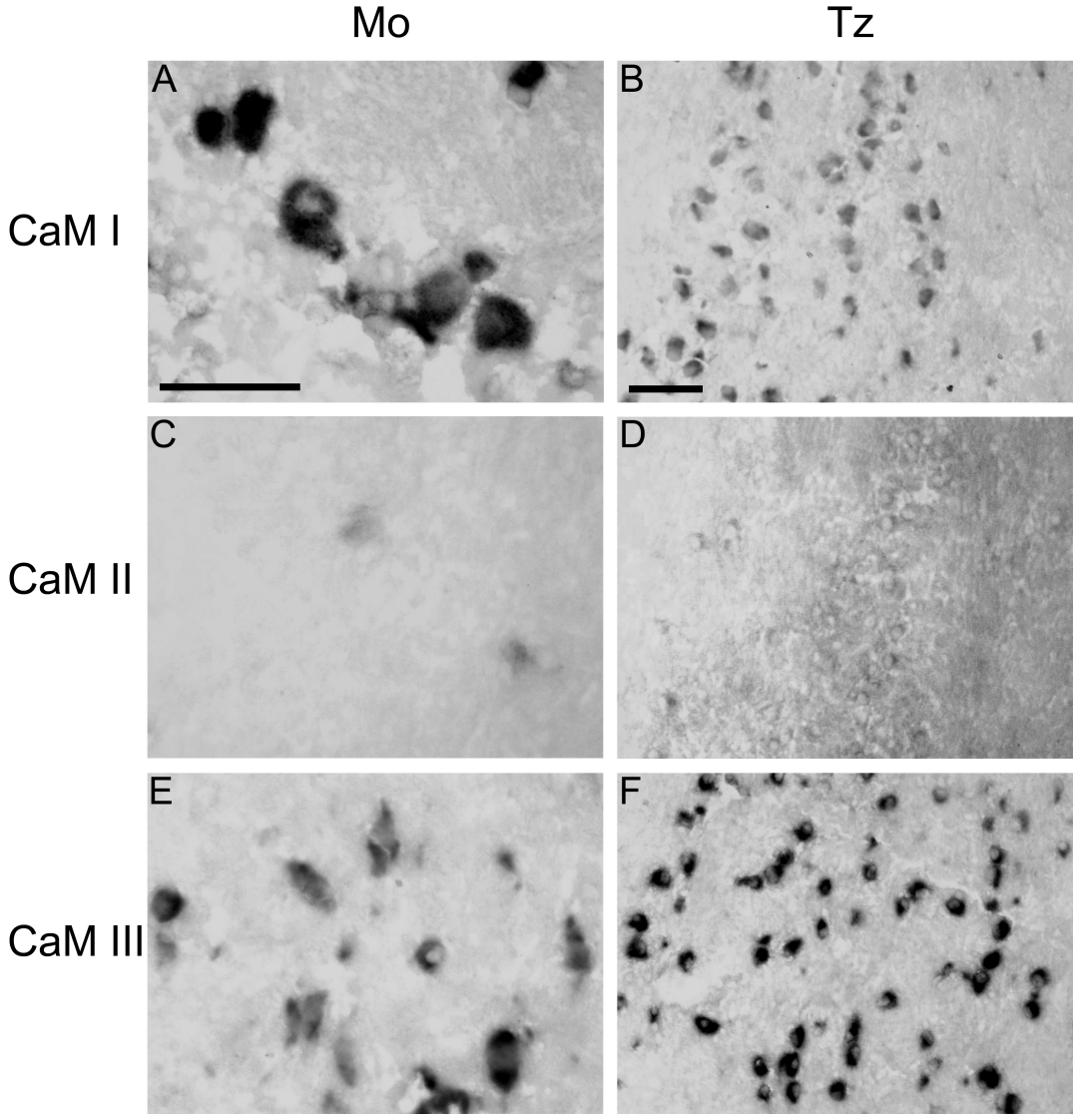


Figure 8. Representative in situ hybridization pictures of DIG-labeled CaM I, II and III gene-specific riboprobes in the motor trigeminal nucleus (Mo5) and the trapezoid body (Tz). The CaM I and III gene expressions are relatively high (A, B, E, F), while low CaM II (C, D) expressions can be seen in both nuclei. Medium-sized cell somata (about 40 μm in diameter) are labeled in the Mo5. The neuropil is generally very low in CaM mRNAs, except in the trapezoid body, where CaM II mRNAs are present in small quantities (D). Scale bars: 100 μm.

A differential CaM gene expression in certain medullar nuclei was also demonstrated. For example, both the Mo5 and the trapezoid body showed a strong preference in expressing the CaM III and CaM I mRNA populations over CaM II mRNAs (Fig. 8E, F). A weak perineuronal label indicating the presence of only a small amount of CaM II mRNA was occasionally seen in these nuclei (Fig. 8C, D).

*5.3. Intranuclear differences in CaM gene expression between the rostral and caudal parts of the individual nuclei of the trigeminal system*

In situ hybridization of [$^{35}$S]-labeled antisense CaM I, II and III cRNA probes to tissue sections of the brain stem–medulla region established a specific and unique distribution of the autoradiographic label (Fig. 9), whereas hybridization with a sense probe (not shown) resulted in very low labeling with nonspecific distribution. The CaM mRNAs transcribed from the three CaM genes were widely distributed, albeit generally with low-to-medium levels, throughout this brain area. Quantitative image analysis of the autoradiograms revealed that the mRNAs transcribed from the CaM III gene were generally most abundant, followed by the CaM I and CaM II mRNA populations (Table 2). This rank order of signal intensity is identical to that reported for other brain (Palfi et al., 1999) and spinal cord areas (Kovacs and Gulya, 2002). The highest specific optical density was detected in the Mo5 for the CaM III transcripts, and the smallest one in the Pr5 for the CaM II gene.

For some CaM genes, significant differences in the amounts of their transcripts were found between the rostral and caudal parts of the individual nuclei of the trigeminal system. In most cases, the CaM gene-specific transcripts were more abundant in the rostral parts of the nuclei, as the levels of mRNAs transcribed from each of the CaM I, II and III genes were significantly higher in the rostral part of the Pr5, while the rostral part of the Mo5 displayed an elevated amount of transcripts for the CaM I gene only. For example, the levels of CaM I transcripts were about 38% and 37% higher in the rostral parts of the Pr5 and the Mo5, respectively. Interestingly, the CaM II mRNAs were most abundant in the caudal part of the Me5.

**Table 2.**

| Component of the trigeminal system | Gene | Average specific gray-scale value (± S.D.) | | % of rostral value |
|---|---|---|---|---|
| | | rostral | caudal | |
| Mesencephalic trigeminal nucleus (Me5) | CaM I | 63.28 ± 11.79 | 64.27 ± 6.95 | 98.46 |
| | CaM II | 56.12 ± 6.67 | 73.33 ± 8.09* | 76.53 |
| | CaM III | 86.31 ± 19.64 | 60.21 ± 8.20 | 143.35 |
| Principal sensory trigeminal nucleus (Pr5) | CaM I | 76.78 ± 6.85 | 55.78 ± 9.33* | 137.65 |
| | CaM II | 43.17 ± 7.72 | 28.86 ± 3.70* | 149.58 |
| | CaM III | 80.87 ± 5.10 | 66.97 ± 6.69* | 120.76 |
| Motor trigeminal nucleus (Mo5) | CaM I | 79.02 ± 7.48 | 57.48 ± 9.84* | 137.47 |
| | CaM II | 38.62 ± 7.55 | 42.13 ± 6.23 | 91.67 |
| | CaM III | 88.22 ± 6.85 | 77.26 ± 8.06 | 114.19 |

Quantitative analysis of CaM gene expression in the trigeminal nuclei of the adult rat brain. Coronal cryostat sections from the pons–medulla area were cut, hybridized separately with antisense [$^{35}$S]cRNA probes specific for CaM I, CaM II or CaM III mRNAs and exposed to autoradiographic film. Film autoradiographic images (at least 4 in each of the 5 animals for a given structure) were analyzed by computer-assisted microdensitometry. Gray-scale levels for each CaM gene were determined by using the image analysis computer program Image J (ver. 1.32). High-resolution gray-scale images were taken and the brain stem structures of interest were outlined on the computer screen. Specific gray-scale values (means of at least 20 measurements from 5 separate experiments ± S.D.) were calculated by subtracting the nonspecific values resulting from the hybridization of the respective sense cRNA probes from the values of the antisense [$^{35}$S]cRNA probes. *Significant differences ($p < 0.05$, two-tailed Student's *t*-test) were found between the rostral and caudal parts of the trigeminal nuclei.

The largest difference between any CaM gene-specific transcript contents of the rostral and caudal parts was found for the CaM II gene in the Pr5, where the levels of these transcripts were otherwise characteristically the lowest. The intranuclear difference here was about 50%, the rostral part being the richer in CaM II mRNAs.

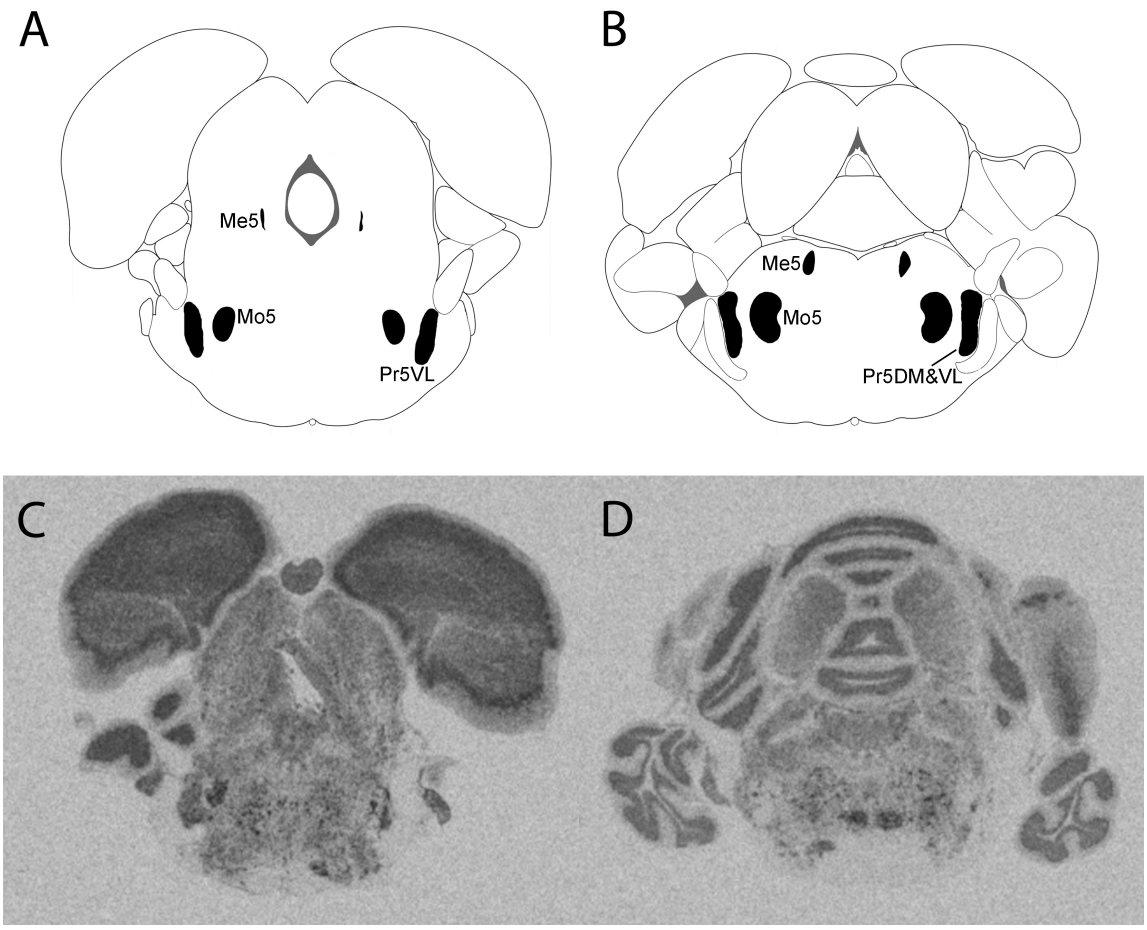


Figure 9. Differential CaM gene expression in the trigeminal nuclei of the rat brain, as evidenced by the specific hybridization of antisense CaM I-gene specific [$^{35}$S]cRNA probes. A, B) Diagrammatic representation of the medullary nuclei (areas labeled solid black) in the rat brain (Paxinos and Watson, 1997). Me5: mesencephalic trigeminal nuclei, Mo5: motor trigeminal nuclei, Pr5VL: principal sensory trigeminal nucleus, ventrolateral part, Pr5DM&VL: principal sensory trigeminal nucleus, dorsomedial and ventrolateral parts. C, D) Specific hybridization of antisense CaM I-gene specific [$^{35}$S]cRNA probes to the coronal sections of the rat brain stem–medulla area. Representative pictures taken from bregma -8.80 mm (C) and -9.30 mm (D), respectively.

*5.4. CaM gene expression in the midbrain–brain stem region after chronic dithranol and/or steroid treatments*

The positions of the trigeminal nuclei in the adult rat brain stem–medulla region investigated in this study are to be seen in Fig. 10. The distribution of multiple CaM mRNA populations was detected by in situ hybridization using CaM gene-specific [$^{35}$S]-labeled riboprobes (Fig. 11). The different parts of the trigeminal system were moderately labeled similarly to other midbrain–brain stem regions, as compared with the more heavily labeled cerebellum. Hybridization with the sense probes resulted in very low labeling (Fig. 2M-O). However, chronic dithranol treatment of the infraorbital skin

selectively affected the CaM gene expression in selected parts of this brain region: an area-dependent and gene-specific differential regulation of CaM gene expression was demonstrated in the Mo5 and the Pr5 of the trigeminal system, of the rat, as evidenced by quantitative in situ hybridization (Figs 11 and 12). Moreover, the CaM gene expression was sensitive to corticosteroid treatment.

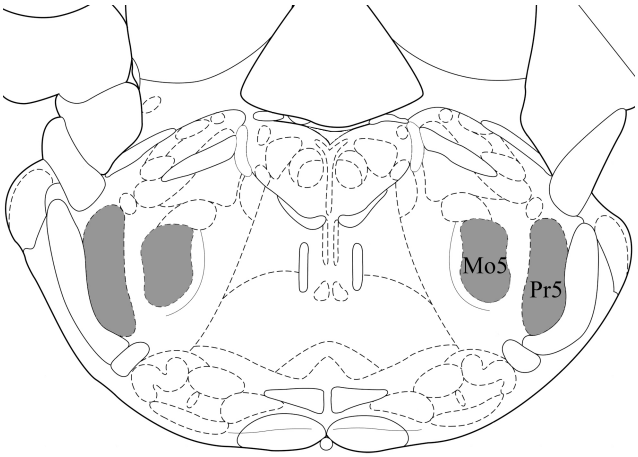


Figure 10. Positions of the trigeminal nuclei in the adult rat brain stem–medulla region investigated in this study (shaded areas, bregma -9.16 mm). Mo5: motor trigeminal nucleus, Pr5: principal sensory trigeminal nucleus.

*5.4.1. CaM gene expression in the Pr5 after chronic dithranol and/or steroid treatments*

In the Pr5, where the neurons postsynaptic to the trigeminal ganglion cells are located, only the CaM II mRNA content increased as a consequence of the 5-day dithranol treatment (by about 30%), while the amounts of the CaM I and III transcripts did not change significantly (Fig. 11D-F). The order of sensitivity of the genes for the chronic dithranol treatment was CaM II > CaM I = CaM III. Subsequent chronic corticosteroid treatment for 5 days was ineffective in lowering the CaM I transcripts in this nucleus.

The most sensitive CaM gene for the subsequent corticosteroid treatment was CaM III, where a 25% increase in the amount of transcripts was observed (Fig. 11I) with virtually unchanged CaM I and CaM II gene expressions (Fig. 11G, H). Chronic corticosteroid treatment administered to the normal infraorbital skin was ineffective in altering the expression of the CaM I gene, but significantly decreased the CaM II and III mRNA populations in this nucleus (Fig. 11J-L). Thus, a differential CaM expression was demonstrated in neurons postsynaptic to those innervating the affected skin region by these treatments (Fig. 12).

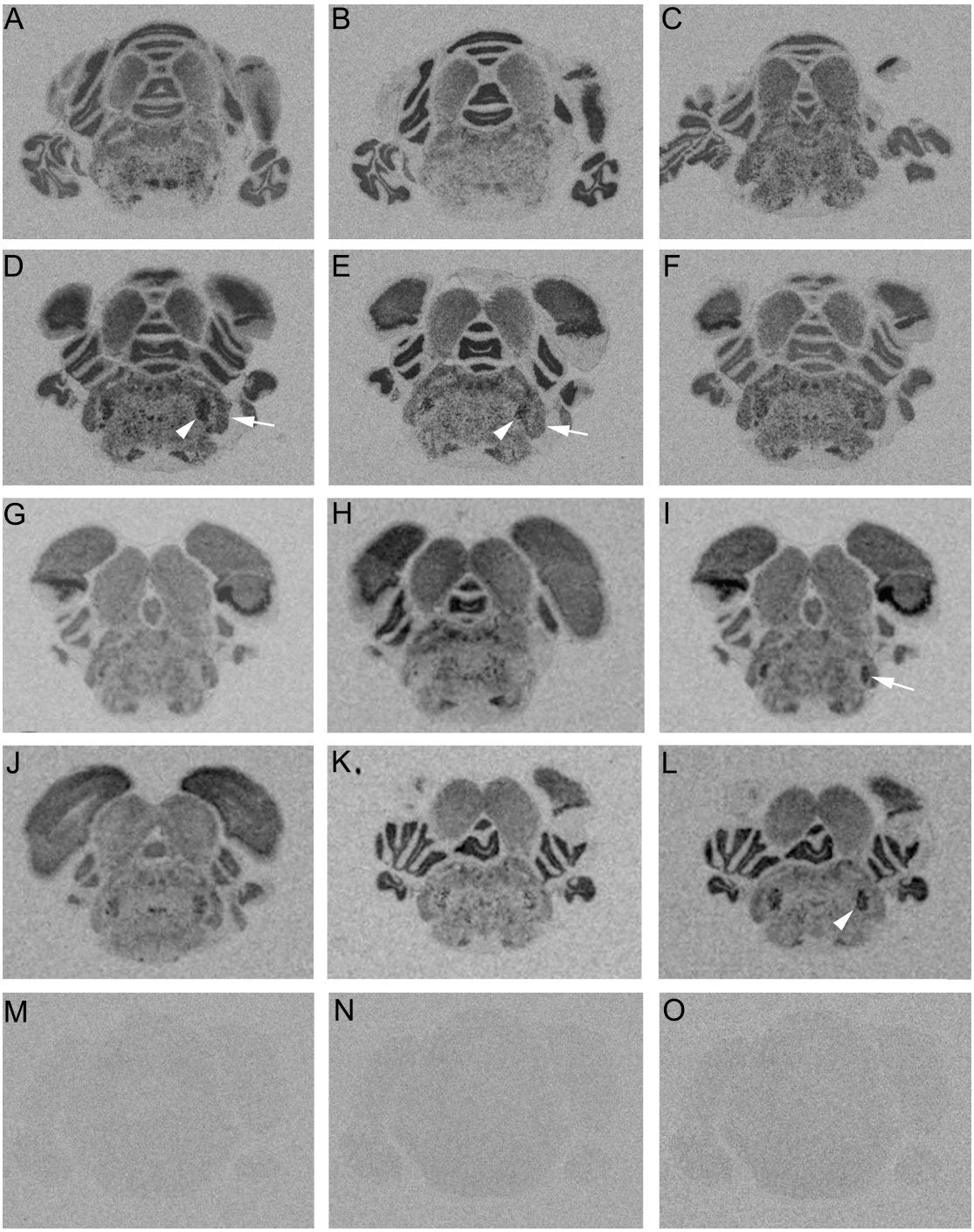


Figure 11. Distribution of multiple CaM mRNA populations as detected by in situ hybridization. A, D, G, J, M: CaM I mRNAs, B, E, H, K, N: CaM II mRNAs, C, F, I, L, O: CaM III mRNAs. A-C: control. D-F: 5-day dithranol treatment. G-I: 5-day dithranol treatment followed by 5-day corticosteroid treatment. J-L: 5-day steroid treatment alone. M-O: sense probes for the CaM I, II and III genes, respectively. White arrows and arrowheads point to the Pr5 and the Mo5, respectively. For example, as seen in panels D and E, 5-day dithranol treatment visibly increased the hybridizable CaM I and II mRNA contents in the Mo5 (arrowheads) and the Pr5 (arrows), respectively. Five-day dithranol treatment followed by 5-day corticosteroid treatment increased the amounts of CaM III transcripts in the Pr5 (arrows, panel I). The 5-day corticosteroid treatment also increased the CaM III mRNAs only in the Mo5 (panel L).

*5.4.2. CaM gene expression in the Mo5 after chronic dithranol and/or steroid treatments*

The amounts of the CaM I and II transcripts increased moderately in the Mo5 as a consequence of the inflammation (Fig. 11D, E and 3). Specifically, after 5 days of treatment, the CaM I and II mRNA contents in this nucleus had increased by about 25% and 20%, respectively, as compared with the controls, while the CaM III mRNAs were not changed significantly (Fig. 11F). The order of sensitivity of the genes for the chronic dithranol treatment in the Mo5 was CaM I > CaM II > CaM III. Subsequent 5-day corticosteroid treatment partially ameliorated the effects of the chronic dithranol-elicited inflammation on the CaM gene expression, as it robustly lowered the amounts of the CaM I and III mRNAs to 40% and 50% of their respective control values (Fig. 11G, I). The CaM gene most sensitive to this treatment regimen was CaM I, followed by CaM III and CaM II. A chronic, 5-day corticosteroid treatment alone elicited different responses in the Mo5: it was either without effect on the CaM I gene expression, or significantly decreased the amounts of the hybridizable CaM II transcripts, or significantly increased the amounts of CaM III transcripts (Fig. 12).

Since a considerable number of neurons in this nucleus are postsynaptic to the sensory neurons located in the Pr5, the changes in CaM expressions seen in the Mo5 are consequences in part of a trans-synaptic regulation, where compensatory events could occur even in the third neuron of the pathway.

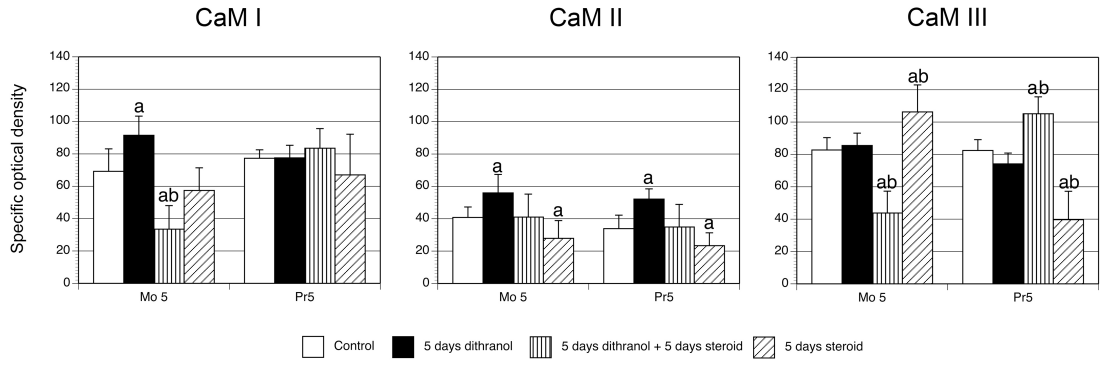


Figure 12. Semiquantitative CaM gene expression pattern analysis during orofacial skin inflammation in the Mo5 and the Pr5. Significant differences ($p < 0.05$) were seen between control vs treated nuclei (a) and between nuclei after 5-day treatment vs 5-day dithranol treatment followed by 5 day-long corticosteroid treatment or corticosteroid treatment alone (b). Mo5: motor trigeminal nucleus, Pr5: principal sensory trigeminal nucleus.

## 6. Discussion

A number of animal models have been designed with the aim of clarifying the cellular and molecular mechanisms involved in the generation of inflammatory pain (Arendt-Nielsen, 1997; Hylden et al., 1989). Most models use chemical irritants or complete Freund adjuvant to elicit acute or chronic inflammation (Carstens et al., 1998; Ikeda et al., 2003; Zhou et al., 1999). Dithranol, an inflammatory agent, is one of the most widely used and effective topical treatments for patients with psoriasis. The molecular basis of its mode of action is still unknown, but it is probably related to the redox activity leading to the production of free radicals (Lambelet et al., 1990; Shroot & Brown, 1986). There are indications that either epidermal proliferation/keratinization or cutaneous inflammation or both may be crucial in the antipsoriatic effect of dithranol; indeed, the often serious inflammation and the irritative response are the most serious limitations for its use (Swinkels et al., 2002c). The extent of such inflammation on the peripheral nerves has previously been demonstrated immunohistochemically through use of the pan-neuronal marker protein UCH-L1 (Doran et al., 1983) in both humans and animals.

### *6.1. Effects of dithranol on ubiquitination, and the consequences on the UCH-L1 immunoreactivity*

The expression of UCH-L1 is highly specific to neurons and to cells of the diffuse neuroendocrine system and their tumors (Doran et al., 1983). The protein is abundant in the nervous system (1-2% of the total protein content of the brain; Wilkinson et al., 1989), where its function is still not completely understood. In vitro, however, UCH-L1 catalyzes the hydrolysis of C-terminal ubiquityl esters and amides (Larsen et al., 1998); this activity is presumed to be critical for cytoplasmic protein degradation. The degradation of proteins via the ubiquitin pathway involves two successive steps: a conjugation of multiple ubiquitin moieties to the substrate, and degradation of the tagged protein by a downstream 26S proteasome complex with the release of ubiquitins. Among the key proteins degraded by the ubiquitin-proteasome system are those involved in the control of inflammation, cell cycle regulation, gene expression and development, and differentiation (Ciechanover et al., 2000; Evans, 2005).

The covalent binding of ubiquitin to proteins normally signals the protein-transport machinery to carry the protein to the proteasome for degradation. This pathway also plays a major role in the breakdown of abnormal proteins that result from a number of causes, including oxidative stress or toxic substances. The UCH-L1 gene is a member of a gene

family whose products remove ubiquitin from ubiquitinated cellular proteins by hydrolyzing small C-terminal adducts of ubiquitin to generate ubiquitin monomers, thereby preventing them from undergoing targeted degradation by the proteasome-dependent pathways. Recent proteomic analysis provided evidence that full-length UCH-L1 is a major target of oxidative damage (Choi et al., 2004) as UCH-L1 can be extensively modified by carbonyl formation and methionine and cysteine oxidation. Thus, impairment of the UCH-L1 ubiquitin hydrolase activity may be an important contributor to the neurodegeneration associated with the accumulation of ubiquitinated proteins and inflammation (Li et al., 2004). In that study, the molecular mechanisms linking inflammation with neurodegeneration were investigated in neuronal cultures. Treatment with certain prostaglandins, which are mediators of inflammation, reduced the viability and increased the levels of ubiquitinated proteins in the neuronal cells.

We demonstrated a complete loss of UCH-L1 immunoreactivity in dithranol-treated orofacial skin after 5 days of dithranol treatment, while the topical application of corticosteroid onto the inflamed skin for 5 days reversed this effect as the UCH-L1 immunoreactivity was almost completely restored; corticosteroid treatment alone, for the same length of time, did not change the appearance of the UCH-L1-immunoreactive nerve fibers (Orojan et al., 2006b). These findings were supported by Western blot analyses. We concluded that dithranol, incidentally similarly as in psoriasis, caused inflammation and abolished UCH-L1 immunoreactivity in the rat orofacial skin in a corticosteroid-reversible manner, and that this phenomenon was due to the ability of dithranol to cause oxidative damage to the UCH-L1 protein, and to the antioxidant activity of the corticosteroids countering this effect. Although the effectiveness of topical corticosteroid treatment in reversing the irritation caused by dithranol had already been revealed (Swinkels et al., 2001, 2003), its ability to restore UCH-L1 immunoreactivity in the skin after inflammation was first demonstrated by our study (Orojan et al., 2006b).

The presence of intracellular aggregates containing ubiquitinated proteins in some of the treated cells indicated that these aggregates can form independently of proteasome inhibition. Impairment of the UCH-L1 ubiquitin hydrolase activity may additionally result in excess ubiquitination of the CaM protein. Indeed, there are observations that support this notion as extensive ubiquitination to the CaM protein, similarly to that of UCH-L1, could also occur as a consequence of the oxidative damage caused by dithranol. It has been shown that CaM is not only a substrate for ubiquitination, as the covalent conjugation of mammalian CaM with ubiquitin was demonstrated in different tissues

(Laub & Jennissen, 1991; Ziegenhagen et al., 1988, 1990), but actively participates in the regulation of the ubiquitination of an ubiquitin-specific protease (Shen et al., 2005).

Dithranol undergoes a complex chemical transformation after topical application. The generation of oxygen free radicals is responsible for both the antipsoriatic and inflammatory effects of the drug (Willis et al., 2001). The experimental data suggest that the oxidative stress generated at the site of dithranol treatment alters the expressions of dermal chemokines and other cytokines, resulting in the recruitment of inflammatory cells (Lange et al., 1998). As dithranol is a powerful tool for the generation of reactive oxidative species in the skin, it is possible that the observed loss of UCH-L1 immunoreactivity in inflamed skin is due to the extensive oxidative damage to the UCH-L1 protein. Previous studies have demonstrated a decrease in UCH-L1 immunoreactivity in several forms of inflammation elicited by bacterial infection (Ge et al., 2002), capsaicin treatment (Simone et al., 1998) or skin diseases of unknown origin, such as lichen planus or lichenoid reactions (Nissalo et al., 2000). Our results show that dithranol-induced inflammation is also a condition that powerfully affects the immunohistochemically detectable amounts of UCH-L1 as it completely eliminates the UCH-L1 immunoreactivity in the nerve fibers in the rat orofacial skin in a corticosteroid-reversible manner. The fact that UCH-L1 immunoreacivity was not completely abolished in the samples used for Western analysis can be explained by 1) the presence of contaminating small amounts of tissue perhaps less affected by dithranol, and 2) the different degrees of accessibility of the epitopes in histological sections and denaturing gel electrophoretic circumstances.

*6.2. Regulation of CaM gene expression in the brain stem–medulla region*

CaM is a ubiquitous, multifunctional cytoplasmic $Ca^{2+}$ receptor protein that is encoded by three different, non-allelic bona fide genes in mammals, and is especially abundant in the CNS, where it plays important roles in a number of $Ca^{2+}$-mediated neuronal functions (for recent reviews, see Palfi et al., 2002; Toutenhoofd & Strehler, 2000) through interactions with a large, heterogenous group of target proteins. CaM exerts its biological action through its target proteins (see Kennedy, 1989; Means, 1991; Palfi et al., 2002, for references). Immunohistochemical and in situ hybridization studies have demonstrated that CaM immunoreactivity or CaM gene-specific riboprobes are often colocalized with target enzymes of CaM. For example, both $Ca^{2+}$/CaM kinase I and IV were present in those retinal layers where the CaM gene expression was most prominent (Kovacs and

Gulya, 2003). Similarly, CaM and many of its target proteins are also colocalized within the same neuronal structures in the pons–brain stem–medulla; $Ca^{2+}$/CaM kinase II or its α and β isoforms (Erondu and Kennedy, 1985; Ochiishi et al., 1998; Ogawa et al., 2005) or the $Ca^{2+}$/CaM-dependent protein phosphatase calcineurin (Strack et al., 1996) are target enzymes of CaM that are probably most frequently noted for their colocalization with CaM in this brain region. For example, multiple lines of evidence suggest that $Ca^{2+}$/CaM kinase II α plays an important role in nociceptive hypersensitivity in the trigeminal sensory neurons (Price et al., 2005), as this enzyme has been shown to modulate the vanilloid receptor type 1. Among the lesser known, or lesser represented target proteins of CaM in this region, the CaM-binding phosphoprotein GAP-43 has been observed in cells in all the major serotonergic and noradrenergic cell groups in the medulla (Wotherspoon et al., 1997). Furthermore, the enzyme $Ca^{2+}$/CaM kinase I has been demonstrated in clusters of neurons and surrounding neuropil throughout the brain stem (Picciotto et al., 1995), and the presence of two isoforms of $Ca^{2+}$/CaM kinase kinases has been revealed in various brain stem nuclei, including the trigeminal nuclei (Sakagami et al., 2000; Okuno et al., 1996). Thus, the colocalization of CaM with many of its target enzymes in the brain stem–medulla region seems to be a general phenomenon.

The regional distribution and expression pattern of the CaM genes in the developing and adult rodent brain have been well documented by in situ hybridization methods (Kortvely et al., 2002; Palfi et al., 1999; Sola et al., 1996). The fact that 3 distinct, non-allelic CaM genes are collectively transcribed into at least 7 transcripts resulting in identical protein products highlights the importance of the (post)transcriptional regulation of these transcripts under normal and (patho)physiological conditions (Palfi and Gulya, 1999; Palfi et al., 2001, 2002; Kortvely and Gulya, 2004; Vizi et al., 2000). The effects of different acute or chronic stimuli employed in these studies on CaM gene expression were generally moderate, rarely larger than 20%, in accordance with the presumed central role of the CaM genes in orchestrating neuronal functions. The distribution of CaM-expressing cells in the brain stem–medulla area of the rat brain was first investigated by our laboratory, and the overall distribution of the different CaM transcripts over relatively large regions was described (Palfi et al., 1999). In our recent, more detailed analyses, we not only provided a more detailed description of the distribution of CaM gene-specific transcripts at the light microscopic level (Orojan et al., 2006a), but were able to detect intranuclear

differences in CaM gene expression profiles in the mesencephalic, motor and principal sensory trigeminal nuclei (Bakota et al., 2005) under physiological conditions.

Similarly to other parts of the CNS, the region of the brain stem–medulla displays a differentially regulated, albeit low-to-medium, CaM gene expression. In general, the most abundant CaM mRNAs were those of the CaM I and III genes. The rank order of CaM mRNA abundance in the brain stem–medulla was similar to that found in many other parts of the CNS (Palfi et al., 1999; Kovacs et al., 2002), where the dominance of CaM I and III transcripts was evident. Moreover, a recent study revealed significant differences in the amounts of the CaM transcripts between the rostral and caudal parts of individual nuclei of the trigeminal system (Bakota et al., 2005); the intranuclear differences seen in the CaM gene expression could be the basis for the somatotopy observed in this region, and could have important functional implications. The differences observed were confined to small areas, pointing to the possibility that higher spatial resolution is needed to map the differentially CaM-expressing cells precisely in this region. For example, Palfi et al. (1999) analyzed 16, mainly large structures in the midbrain–brain stem area, 5 of which displayed significantly different CaM gene expressions. The relatively low spatial resolution of the film autoradiography used in that study might have resulted in obscured smaller areas with distinct differential CaM gene expressions; this prompted us to revisit this issue, and investigate the gene expression pattern in much smaller regions. Our results show (Orojan et al., 2006a) that even small regions, such as the trigeminal system, exhibit significantly different distributions of [$^{35}$S]- and DIG-labeled CaM gene-specific transcripts. We believe that the localization and quantitative analysis of the CaM gene expression in the brain stem–medulla region presented in our studies could facilitate our understanding of the roles this protein plays via its target enzymes in the numerous functional aspects related to this brain area.

Among the cranial nerves that carry sensory information to the CNS, the rodent trigeminal system is of special interest because of its precise somatotopic organization (Waite, 1984; Waite and Tracey, 1995). The trigeminal sensory nuclei are divided into three groups: the mesencephalic nucleus (Me5), the principal sensory nucleus (Pr5), and the spinal trigeminal nucleus (Sp5), this latter being subdivided into the nucleus spinal subnuclei oralis (Sp5O), the nucleus interpolaris (Sp5I) and the nucleus caudalis (Sp5C). The organization of terminations in the main and spinal nuclei is most clearly evident for vibrissal afferents, for which a pattern analogous to the peripheral arrangement of vibrissae can be discerned in coronal sections. Each vibrissa is associated with a patch or

barrel (for references, see Waite and Tracey, 1995). In general, three representations of the vibrissae are seen, in the Pr5, Sp5I and Sp5C; although the Sp5O receives vibrissal terminations, no patches are evident in this subnucleus. In the horizontal plane, terminations from each vibrissa are seen as long rostrocaudal columns throughout the nuclei in a somatotopic pattern. The presence of the somatotopic pattern of the rostrocaudal barrels is most evident for the Pr5. Our CaM expression data (Orojan et al., 2008) could be interpreted as showing a differential CaM mRNA distribution along the rostrocaudal axis of this nucleus, which is a consequence of the separate information received from the rostral and caudal vibrissal fields.

The Mo5 of the rat is divided into a large dorsolateral division extending throughout the rostrocaudal length of the nucleus and a smaller ventromedial division in the caudal two-thirds (for references, see Travers, 1995). The jaw-closing muscles, the masseter, the temporalis and the medial pterygoid, are innervated from the dorsolateral division, while two jaw-opening muscles, the anterior digastric and the mylohyoid, are innervated from the ventrolateral division. A third jaw-opening muscle, the lateral pterygoid, is grouped together with jaw-closing motoneurons in the ventral aspect of the dorsoventral division. Even though the areas corresponding to the dorsolateral and ventromedial divisions are not distinguishable on the basis of their CaM gene expression patterns in the coronal sections of the caudal part of the nucleus, the caudal part nevertheless clearly has higher levels of CaM mRNA populations.

The major organizing principles of the vertebrate CNS determine that its parts receive inputs from separate sources, while separate efferent connections project to different neuroanatomical entities. Previous studies have established that certain nuclei in the central nervous system display a differential structural and functional organization, mainly along their rostrocaudal axis, that can be seen in the differences in their neuronal circuitry, neurochemical cytoarchitecture or gene expression pattern. This somatotopy is also present in the brain stem, one of the nuclei most characteristically expressing this feature being the parabrachial nucleus (PBN). The PBN has been divided into at least 13 distinct subnuclei and regions, each associated with a unique set of afferents, efferents and neurotransmitters (for references, see Saper, 1995), which frequently mark out distinct terminal fields according to their receptive fields. For example, projections to the PBN from the nucleus of the solitary tract carry afferent signals from both the oral cavity and the gastrointestinal tract. Although physiological studies have suggested the convergence of oral and gastrointestinal sensory signals in the PBN, anatomical studies

have emphasized the segregation of these pathways in the rat. Karimnamazi et al. (2002) found that the gastric terminations in the PBN were separate from the taste projections in the rostral portion of the external lateral and dorsal lateral subnuclei, while the gustatory projections were separate from the gastric terminations in the ventral lateral and central medial subnuclei of the caudal “waist” region, and were intermingled with the gastric projections in these subnuclei and the external subnuclei at slightly more rostral levels. The physiological evidence for overlap in the PBN was also evaluated, as neurophysiological recordings demonstrated that a small proportion of single cells within the waist and external subnuclei could be activated by both gastric and orotactile stimulation. The behavioral roles of the "waist" area and external subnuclei of the PBN in the processing of gustatory information have also been defined by monitoring oromotor behavior in the areas within and surrounding this nucleus (Galvin et al., 2004). Electrical and chemical stimulation of the “waist” area increased ingestive oromotor behavior, while stimulation of the external parabrachial subnuclei and areas medial and ventral to the nucleus did not result in a behavioral change. These data supported the hypothesis that the waist area of the PBN constitutes part of the neural substrate involved in eliciting oromotor behavior in response to taste input. However, another experiment (Gulya et al., 1991) provided indirect evidence for the separation of functions within a nucleus that resides outside the brain stem. It was reported that the vasopressin-containing cells in the bed nucleus of the stria terminalis responded to dehydration and/or to ethanol treatment in a subregion-dependent manner within the nucleus. Dehydration affected only cells in the central (or medial) region, while ethanol ingestion also affected cells in the caudal region of the nucleus. As the different parts of this nucleus send afferents both to the lateral septum and to the neurohypophysis in rodents (Kelly and Swanson, 1980), or to several regions of the mesencephalon, pons and medulla oblongata in the cat (Holstege et al., 1985), the anatomical basis for the segregation of functions, involving the differential regulation of vasopressin gene expression, is plausible.

In the present study, a brain area-dependent, differential CaM gene expression was described after the eliciting of chronic peripheral inflammation and subsequent corticosteroid treatment. Corticosteroid treatment alone was also effective in eliciting differential CaM gene expression in these nuclei. The responses were dependent on the afferent neuronal connections of these nuclei, as neurons within the trigeminal ganglion supply relatively localized regions of the skin (e.g. the maxillary division), and project to the central parts of the Pr5 and more caudally to the spinal subnucleus caudalis (Waite

and Tracey, 1995). Since a subgroup of neurons of the Pr5 projects to the Mo5 (Travers and Norgren, 1983), and the orofacial region investigated in this study contains some muscles (the anterior and posterior segments of the deep masseter muscle), a trans-synaptically acting regulation of the CaM gene expression elicited by dithranol treatment or steroid modulation cannot be ruled out. Thus, CaM gene expression in the Mo5 could be affected by either or both of the pathways in which the infraorbital area of the orofacial skin is connected to this nucleus. The motor innervation of the vibrissa pad is supplied by the neurons of the facial nucleus (Travers, 1995), a CNS area not involved in this study. Other muscles (e.g. the buccinator and the orbicularis oculi) and the intrinsic muscles of the vibrissae, all situated in the infraorbital region, are innervated instead by neurons located in the facial nerve (Waite and Tracey, 1995). Some of the neurotransmitters in these nuclei have already been identified: acetylcholine, cholecystokinin, and calcitonin gene-related peptide for the Mo5 (for references, see Travers, 1995), and GABA and glutamate for the Pr5 (for references, see Waite and Tracey, 1995).

Beneficial effects of steroids (estrogens, catecholestrogens, phytoestrogens, dehydroepiandrosterone, 7α-hydroxy-dehydroepiandrosterone, etc.) in preventing oxidative stress-associated tissue injury have been observed in different experimental models (Gagne et al., 2003; Munoz-Castaneda et al., 2006; Pelissier et al., 2006), and the effectiveness of antioxidants against dithranol-associated toxicities has been successfully demonstrated (Lange et al., 1998; Swinkels et al., 2001, 2003). Our results show that corticosteroid treatment ameliorates dithranol-induced inflammation, as it attenuates the oxidative damage to UCH-L1, which leads to the reappearance of its immunohistochemically detectable form. Steroids are also potent modulators of gene expression in the nervous tissue (Morsink et al., 2006; Qin et al., 2003). More specifically, corticosteroids differentially regulate CaM gene expression (Das et al., 2000; Morsink et al., 2006). For example, adrenalectomy selectively attenuates the levels of CaM III, but not CaM I or CaM II mRNAs in both the cerebral cortex and the hippocampus, while corticosteroid treatment prevents the effects of adrenalectomy on these genes (Gannon & McEwen, 1994). In recent large-scale gene expression profiling studies involving the serial analysis of gene expression (SAGE; Morsink et al., 2006) showed that the CaM II gene was down-regulated after corticosteroid treatment in hippocampal slice cultures, while Nishida et al. (2006) provided evidence for a reduction

of the CaM I mRNA level and for an expressed sequence tag similar to CaM II (EST CaM II) in the hypothalamus.

## 7. Conclusions

Our results draw attention to a possible causal relation between the differences in afferent and efferent neuronal connections (and consequently in their presumably segregated functions) of the rostral and caudal parts of the trigeminal nuclei and their differential CaM gene expression. In light of the above data, our present findings can be interpreted as trans-synaptic regulatory responses of the CaM gene expression to two opposing effects: the effect of dithranol in degrading proteins that include CaM and the deubiquitinating protein UCH-L1 itself, via its production of free radicals, which result in a differentially altered CaM gene expression; and the modulatory (generally inhibitory) effect of the corticosteroids on the CaM gene expression, resulting in a decreased transcription of the CaM genes. These data provide evidence that chronic inflammation and subsequent corticosteroid treatment can influence the neuronal CaM gene expression through multiple synaptic contacts. Long-lasting changes elicited in the periphery by chronic noxious stimuli (e.g. inflammatory processes or their treatment with steroids) through the peripheral nerves could elicit alterations in, and therefore influence, the CNS functions. These stressors may be important components in the regulatory mechanisms of neuronal gene expression as they could result in transneuronal plasticity, where compensatory increases or decreases in the multiple CaM genes occur in the Pr5 and Mo5.

Collectively, these findings suggest that the differential regulation of the CaM genes in these projection sites are ipsilaterally and trans-synaptically modulated, perhaps via multiple signaling pathways. However, the precise molecular mechanisms underlying this often opposing regulation are unknown.

## 8. Acknowledgments

This research was supported by grants from the National Scientific Research Fund (OTKA, Hungary, T034621), and from the Regional Neurobiology Knowledge Center (RET006) to K.G.

I am grateful to Professor Karoly Gulya, Head of the Department of Cell Biology and Molecular Medicine (formerly the Department of Zoology and Cell Biology), for his continuous support and encouragement, and for providing me with the opportunity to

carry out my research at his Department. I am also grateful to my coworkers, Dr. Lidia Bakota, Szilvia Varszegi and Csaba Szigeti, for their support and help during my research. I am especially indebted to Mrs. Susan Ambrus and Mr. Laszlo Kalman for their excellent technical help.

Finally, for their indispensable help and love, I would like to thank my whole family, to whom I dedicate this work.

## 9. References

Al'Abadie MS, Senior HJ, Bleehen SS, Gawkrodger DJ (1995) Neuropeptides and general neuronal marker in psoriasis – an immunohistochemical study. Clin Exp Dermatol 20:384-389.

Arendt-Nielsen L (1997) Induction and assessment of experimental pain from human skin, muscle, and viscera. In: Jensen, T. S., Turner, J. A., Wiesenfeld-Hallin, Z., (Eds) Proceedings of the 8th World Congress on Pain, Seattle, USA. IASP Press Progr Pain Res Managem 8:393-425.

Bakota L, Orojan I, Gulya K (2005) Intranuclear differences in calmodulin gene expression in the trigeminal nuclei of the rat brain. Acta Biol Szeged 49:9-14.

Bruggemann I, Schulz S, Wiborny D, Hollt V (2000) Colocalization of the mu-opioid receptor and calcium/calmodulin-dependent kinase II in distinct pain-processing brain regions. Mol Brain Res 85:239-250.

Caceres A, Bender P, Snavely L, Rebhun LI, Steward O (1983) Distribution and subcellular localization of calmodulin in adult and developing brain tissue. Neurosci 10:449-461.

Carstens E, Kuenzler N, Handwerker HO (1998) Activation of neurons in rat trigeminal subnucleus caudalis by different irritant chemicals applied to oral or ocular mucosa. J Neurophysiol 80:465-492.

Choi J, Levey AI, Weintraub ST, Rees HD, Gearing M, Chin LS, Li L (2004) Oxidative modifications and down-regulation of ubiquitin carboxyl-terminal hydrolase L1 associated with idiopathic Parkinson's and Alzheimer's diseases. J biol Chem 279:13256-13264.

Ciechanover A, Orian A, Schwartz AL (2000) The ubiquitin-mediated proteolytic pathway: mode of action and clinical implications. J Cell Biochem Suppl 34:40-51.

Das SK, Tan J, Raja S, Halder J, Paria BC, Dey SK (2000) Estrogen targets genes involved in protein processing, calcium homeostasis, and Wnt signaling in the mouse uterus independent of estrogen receptor-α and -β. J biol Chem 275:28834-28842.

Doran JF, Jackson P, Kynoch PA, Thompson RJ (1983) Isolation of PGP 9.5, a new human neuron-specific protein detected by high-resolution two-dimesional electrophoresis. J Neurochem 40:1542-1547.

Dun RB (1958) Growth of the mouse coat. Aust J Biol Sci 11:95-105.

Erondu NE, Kennedy MB (1985) Regional distribution of type II $Ca^{2+}$/calmodulin-dependent protein kinase in rat brain. J Neurosci 5:3270-3277.

Evans PC (2005) Regulation of pro-inflammatory signalling networks by ubiquitin: identification of novel targets for anti-inflammatory drugs. Expert Rev Mol Med 7:1-19.

Facer P, Mann D, Mathur R, Pandya S, Ladiwala U, Singhal B, Hongo J, Sinicropi DV, Terenghi G, Anand P (2000) Do nerve growth factor-related mechanisms contribute to loss of cutaneous nociception in leprosy? Pain 85:231-238.

Fukushima T, Kerr FWL (1979) Organization of trigemino-thalamic tracts and other thalamic afferent systems of the brainstem in the rat: Presence of gelatinosa neurons with thalamic connections. J comp Neurol 183:169-184.

Gagne B, Gelinas S, Bureau G, Lagace B, Ramassamy C, Chiasson K, Valastro B, Martinoli MG (2003) Effects of estradiol, phytoestrogens, and Ginkgo biloba extracts against 1-methyl-4-phenyl-pyridine-induced oxidative stress. Endocrine 21:89-95.

Galvin KE, King CT, King MS (2004) Stimulation of specific regions of the parabrachial nucleus elicits ingestive oromotor behaviors in conscious rats. Behav Neurosci 118:163-172.

Gannon MN, McEwen BS (1994) Distribution and regulation of calmodulin mRNAs in rat brain. Mol Brain Res 22:186-192.

Ge Y, Tsukatani T, Nishimura T, Furukawa M, MiwaT (2002) Cell death of olfactory receptor neurons in a rat with nasosinusitis infected artificially with Staphylococcus. Chem Senses 27:521-527.

Gulya K, Dave JR, Hoffman PL (1991) Chronic ethanol ingestion decreases vasopressin mRNA in hypothalamic and extrahypothalamic nuclei of mouse brain. Brain Res 557:129-135.

Hagforsen E, Nordlind K, Michaelsson G (2000) Skin nerve fibres and their contacts with mast cells in patients with palmoplantar pustulosis. Arch Dermatol Res 292:269-274.

Holstege G, Meiners L, Tan K (1985) Projections of the bed nucleus of the stria terminalis to the mesencephalon, pons, and medulla oblongata in the cat. Exp Brain Res 58:379-91.

Hylden JL, Nahin RL, Traub RJ, Dubner R (1989) Expansion of receptive fields of spinal lamina I projection neurons in rats with unilateral adjuvant-induced inflammation: The contribution of dorsal horn mechanisms. Pain 37:229–243.

Ichikawa H, Gouty S, Regalia J, Helke CJ, Sugimoto T (2004) $Ca^{2+}$/calmodulin-dependent protein kinase II in the rat cranial sensory ganglia. Brain Res 1005:36-43.

Ikeda T, Terayama R, Jue SS, Sugiyo S, Dubner R, Ren K (2003) Differential rostral projections of caudal brainstem neurons receiving trigeminal input after masseter inflammation. J comp Neurol 465:220-233.

Johansson O, Han S-W, Enhamre A (1991) Altered cutaneous innervation in psoriatic skin as revealed by PGP 9.5 immunohistochemistry. Arch Dermatol Res 283:519-523.

Karimnamazi H, Travers SP, Travers JB (2002) Oral and gastric input to the parabrachial nucleus of the rat. Brain Res 957:193-206.

Kelly J, Swanson LW (1980) Additional forebrain regions projecting to the posterior pituitary: preoptic region, bed nucleus of the stria terminalis, and zona incerta. Brain Res 197:1-9.

Kennedy MB (1989) Regulation of neuronal function by calcium. Trends Neurosci 12:417-420.

Kortvely E, Palfi A, Bakota L, Gulya K (2002) Ontogeny of calmodulin gene expression in rat brain. Neurosci 114:301-316.

Kortvely E, Varszegi S, Palfi A, Gulya K (2003) Intracellular targeting of calmodulin mRNAs in primary hippocampal cells. J Histochem Cytochem 51:541-544.

Kortvely E. Gulya K (2004) Calmodulin, and various ways to regulate its activity. Life Sci 74:1065-1070.

Kovacs B, Gulya K (2002) Differential expression of multiple calmodulin genes in cells of the white matter of the rat spinal cord. Mol Brain Res 102:28-34.

Kovacs B, Gulya K (2003) Calmodulin gene expression in the neural retina of the adult rat. Life Sci 73:3213-3224.

Lambelet P, Ducret F, Loliger J, Maignan J, Reichert U, Shroot B (1990) The relevance of secondary radicals in the mode of action of anthralin. Free Radical Biol Med 9:183-190.

Lange RW, Germolec DR, Foley JF, Luster MI (1998) Antioxidants attennuate anthralin-induced skin inflammation in BALB/c mice: role of specific proinflammatory cytokines. J Leukoc Biol 64:170-176.

Larsen CN, Krantz BA, Wilkinson KD (1998) Substrate specificity of deubiquitinating enzymes: ubiquitin C-terminal hydrolases. Biochemistry 37:3358-3368.

Laub M, Jennissen HP (1991) Ubiquitination of endogenous calmodulin in rabbit tissue extracts. FEBS Lett 294:229-233.

Li Z, Melandri F, Berdo I, Jansen M, Hunter L, Wright S, Valbrun D, Figueiredo-Pereira ME (2004) Delta12-prostaglandin J2 inhibits the ubiquitin hydrolase UCH-L1 and elicits ubiquitin-protein aggregation without proteasome inhibition. Biochem Biophys Res Comm 319:1171-1180.

Liu L, Simon SA (2003) Modulation of IA currents by capsaicin in rat trigeminal ganglion neurons. J Neurophysiol 89:1387-1401.

Lowry OH, Rosebrough NJ, Farr AL, Randall RJ (1951) Protein measurement with the Folin phenol reagent. J biol Chem 193:265-275.

McBride SR, Walker P, Reynolds NJ (2003) Optimizing the frequency of outpatient short-contact dithranol treatment used in combination with broadband ultraviolet B for psoriasis: a randomized, within-patient controlled trial. Br J Dermatol 149:1259-1265.

McGill A, Frank A, Emmett N, Turnbull DM, Birch-Machin MA, Reynolds NJ (2005) The anti-psoriatic drug anthralin accumulates in keratinocyte mitochondria, dissipates mitochondrial membrane potential, and induces apoptosis through a pathway dependent on respiratory competent mitochondria. FASEB J 19:1012-1014.

McGrouther DA, Ahmad FS (1998) A preliminary report: the changes in the neuropeptide containing epidermal innervation in response to inflammatory reactions elicited in human breast skin. J R Coll Surg Edinb 43:49-52.

Means AR, VanBerkum MF, Bagchi I, Lu KP, Rasmussen CD (1991) Regulatory functions of calmodulin. Pharmacol Ther 50:255-270.

Morsink MC, Steenbergen PJ, Vos JB, Karst H, Joels M, De Kloet ER, Datson NA (2006) Acute activation of hippocampal glucocorticoid receptors results in different waves of gene expression throughout time. J Neuroendocrinol 18:239-252.

Munoz-Castaneda JR, Muntane J, Munoz MC, Bujalance I, Montilla P, Tunez I (2006) Estradiol and catecholestrogens protect against adriamycin-induced oxidative stress in erythrocytes of ovariectomized rats. Toxicol Lett 160:196-203.

Ni B, Landry CF, Brown IR (1992) Developmental expression of neuronal calmodulin mRNA species in the rat brain analyzed by in situ hybridization. J Neurosci Res 33:559-567.

Nishida Y, Yoshioka M, St-Amand J (2006) Regulation of hypothalamic gene expression by glucocorticoid: implications for energy homeostasis. Physiol Genomics 25:96-104.

Nissalo S, Hietanen J, Malmstrom M, Hukkanen M, Polak J, Konttinen YT (2000) Disorder-specific changes in innervation in oral lichen planus and lichenoid reactions. J Oral Pathol Med 29:361-369.

Nojima H (1989) Structural organization of multiple rat calmodulin genes. J Mol Biol 208:269-282.

Nojima H, Sokabe H (1987) Structure of a gene for rat calmodulin. J Mol Biol 193:439-445.

Ochiishi T, Yamauchi T, Terashima T (1998) Regional differences between the immunohistochemical distribution of $Ca^{2+}$/calmodulin-dependent protein kinase II alpha and beta isoforms in the brainstem of the rat. Brain Res 790:129-140.

Ogawa A, Dai Y, Yamanaka H, Iwata K, Niwa H, Noguchi K (2005) Ca($^{2+}$)/calmodulin-protein kinase IIalpha in the trigeminal subnucleus caudalis contributes to neuropathic pain following inferior alveolar nerve transection. Exp Neurol 192:310-319.

Okuno S, Kitani T, Fujisawa H (1996) Evidence for the existence of $Ca^{2+}$/calmodulin-dependent protein kinase IV kinase isoforms in rat brain. J Biochem (Tokyo) 119:1176-1181.

Orojan I, Bakota L, Gulya K (2006a) Differential calmodulin gene expression in the nuclei of the rat midbrain-brain stem region. Acta Histochem 108:455-462.

Orojan I, Bakota L, Gulya K (2008) Trans-synaptic regulation of calmodulin gene expression after experimentally induced orofacial inflammation and subsequent

corticosteroid treatment in the principal sensory and motor trigeminal nuclei of the rat. Neurochem Int 52:265-271.

Orojan I, Szigeti C, Varszegi S, Gulya K (2006b) Dithranol abolishes UCH-L1 immunoreactivity in the nerve fibers of the rat orofacial skin. Brain Res 1121:216-220.

Palfi A, Gulya K (1999) Water deprivation upregulates the three calmodulin genes in exclusively the supraoptic nucleus of the rat brain. Mol Brain Res 74:111-116.

Palfi A, Hatvani L, Gulya K (1998) A new quantitative film autoradiographic method of quantifying mRNA transcripts for in situ hybridization. J Histochem Cytochem 46:1141-1149.

Palfi A, Kortvely E, Fekete E, Gulya K (2005) Multiple calmodulin mRNAs are selectively transported to functionally different neuronal and glial compartments in the rat hippocampus. An electron microscopic in situ hybridization study. Life Sci 77:1405-1415.

Palfi A, Kortvely E, Fekete E, Kovacs B, Varszegi S, Gulya K (2002) Differential calmodulin gene expression in the rodent brain. Life Sci 70:2829-2855.

Palfi A, Simonka JA, Pataricza M, Tekulics P, Lepran I, Papp G, Gulya K (2001) Postischemic calmodulin gene expression in the rat hippocampus. Life Sci 68:2373-2381.

Palfi A, Vizi S, Gulya K (1999) Differential distribution and intracellular targeting of mRNAs corresponding to the three calmodulin genes in rat brain: a quantitative in situ hybridization study. J Histochem Cytochem 47:583-600.

Paxinos G, Watson C (1997). The rat brain in stereotaxic coordinates, 3rd ed. Academic Press, San Diego.

Pelissier MA, Muller C, Hill M, Morfin R (2006) Protection against dextran sodium sulfate-induced colitis by dehydroepiandrosterone and 7alpha-hydroxy-dehydroepiandrosterone in the rat. Steroids 71:240-248.

Picciotto MR, Zoli M, Bertuzzi G, Nairn AC (1995) Immunochemical localization of calcium/calmodulin-dependent protein kinase I. Synapse 20:75-84.

Poli E, Lazzaretti M, Grandi D, Pozzoli C, Coruzzi G (2001) Morphological and functional alterations of the myenteric plexus in rats with TNBS-induced colitis. Neurochem Res 26:1085-1093.

Price TJ, Jeske NA, Flores CM, Hargreaves KM (2005) Pharmacological interactions between calcium/calmodulin-dependent kinase II alpha and TRPV1 receptors in rat trigeminal sensory neurons. Neurosci Lett 389:94-98.

Qin Y, Nair S, Karst H, Vreugdenhil E, Datson N, Joels M (2003) Gene expression changes in single dentate granule neurons after adrenalectomy of rats. Mol Brain Res 111:17-23.

Rice FL, Manse A, Munger BL (1986) A comparative light microscopic analysis of sensory innervation of the mystacial pad. I. Innervation of vibrissal follicle-sinus complexes. J comp Neurol 252:154-174.

Sakagami H, Umemiya M, Saito S, Kondo H (2000) Distinct immunohistochemical localization of two isoforms of $Ca^{2+}$/calmodulin-dependent protein kinase kinases in the adult rat brain. Eur J Neurosci 12:89-99.

Saper CB (1995) Central autonomic system. In: The rat nervous system. ed., Paxinos G. Second ed. Academic Press, San Diego, pp. 107-135.

Seto-Ohshima A, Kitajima S, Sano M, Kato K, Mizutani A (1983) Immunohistochemical localization of calmodulin in mouse brain. Histochem 79:251-257.

Seto-Ohshima A, Yamazaki Y, Kawamura N, Sano M, Kitajima S, Mizutani A (1987) The early expression of immunoreactivity for calmodulin in the nervous system of mouse embryos. Histochem 86:337-343.

Shen C, Ye Y, Robertson SE, Lau AW, Mak DO, Chou MM (2005) Calcium/calmodulin regulates ubiquitination of the ubiquitin-specific protease TRE17/USP6. J biol Chem 280:35967-35973.

Shroot B, Brown C (1986) Free radicals in skin exposed to dithranol and its derivatives. Arzneilmittelforsch 36:1253-1255.

Simone DA, Nolano M, Johnson T, Wendelschafer-Crabb G, Kennedy WR (1998) Intradermal injection of capsaicin in humans produces degeneration and subsequent reinnervation of epidermal nerve fibers: correlation with sensory function. J Neurosci 18:8947-8959.

Sola C, Tusell JM, Serratosa J (1996) Comparative study of the pattern of expression of calmodulin messenger RNAs in the mouse brain. Neurosci 75:245–256.

Steinhoff M, Stander S, Seeliger S, Ansel JC, Schmelz M, Luger T (2003) Modern aspects of cutaneous neurogenic inflammation. Arch Dermatol 139:1479-1488.

Strack S, Wadzinski BE, Ebner FF (1996) Localization of the calcium/calmodulin-dependent protein phosphatase, calcineurin, in the hindbrain and spinal cord of the rat. J comp Neurol 375:66-76.

Swinkels OQ, Kucharekova M, Prins M, Gerritsen MJ, van der Valk PG, van de Kerkhof PC (2003) The effects of topical corticosteroids and a coal tar preparation on dithranol-induced irritation in patients with psoriasis. Skin Pharmacol Appl Skin Physiol 16:12-17.

Swinkels OQ, Prins M, Birker LW, Gerritsen MJ, van der Valk PG, van de Kerkhof PC (2002a) The response of normal human skin to single and repeated applications of dithranol cream: an immunohistochemical assessment. Skin Pharmacol Appl Skin Physiol 15:262-269.

Swinkels OQ, Prins M, Gerritsen MJ, van Vlijmen-Willems IM, van der Valk PG, van de Kerkhof PC (2002b) An immunohistochemical assessment of the response of the psoriatic lesion to single and repeated applications of high-dose dithranol cream. Skin Pharmacol Appl Skin Physiol 15:393-400.

Swinkels OQ, Prins M, Tosserams EF, Gerritsen MJ, van Der Valk PG, van de Kerkhof PC (2001) The influence of a topical corticosteroid on short-contact high-dose dithranol therapy. Br J Dermatol 145:63-69.

Swinkels OQ, Prins M, van Vlijmen-Willems IM, Gerritsen MJ, van der Valk PG, van de Kerkhof PC (2002c) The response of uninvolved skin of patients with psoriasis to single and repeated applications of dithranol cream: an immunohistochemical assessment. Skin Pharmacol Appl Skin Physiol 15:385-392.

Toutenhoofd SL, Strehler EE (2000) The calmodulin multigene family as a unique case of genetic redundancy: multiple levels of regulation to provide spatial and temporal control of calmodulin pools? Cell Calcium 28:83-96.

Travers JB (1995) Oromotor nuclei. In The rat nervous system. ed., Paxinos G. Second ed. Academic Press, San Diego, pp. 239-255.

Travers JB, Norgren R (1983) Afferent projections to the oral motor nuclei of the rat. J comp Neurol 220:280-298.

van de Kerkhof PC, Franssen ME (2001) Psoriasis of the scalp. Diagnosis and management. Am J Clin Dermatol 2:159-165.

van der Loos H, Dorfl J, Welker E (1984) Variation in pattern of mystacial vibrissae in mice. J Hered 75:326-336.

van der Vleuten CJ, de Jong EM, van de Kerkhof PC (1996) Epidermal differentiation characteristics of the psoriatic plaque during short contact treatment with dithranol cream. Clin Exp Dermatol 21:409-414.

Vizi S, Palfi A, Gulya K (2000) Multiple calmodulin genes exhibit systematically differential responses to chronic ethanol treatment and withdrawal in several regions of the rat brain. Mol Brain Res 83:63-71.

Vizi S, Palfi A, Hatvani L, Gulya K (2001) Methods for quantification of in situ hybridization signals obtained by film autoradiography and phosphorimaging applied for estimation of regional levels of calmodulin mRNA classes in the rat brain. Brain Res Protoc 8:32-44.

Waite PME (1984) Rearrangement of neuronal responses in the trigeminal system of the rat following peripheral nerve section. J Physiol (Lond) 352:425-445.

Waite PME, Tracey DJ (1995) Trigeminal sensory system. In: The rat nervous system. ed., Paxinos G. Second ed. Academic Press, San Diego, pp. 705-724.

Wilkinson KD, Lee KM, Deshpande S, Duerksen-Hughes P, Boss JM, Pohl J (1989) The neuron-specific protein PGP 9.5 is a ubiquitin carboxyl-terminal hydrolase. Science 246:670-673.

Willis CM, Britton LE, Reiche L, Wilkinson JD (2001) Reduced levels of glutathione S-transferases in patch test reactions to dithranol and sodium lauryl sulphate as demonstrated by quantitative immunocytochemistry: evidence for oxidative stress in acute irritant contact dermatitis. Eur J Dermatol 11:99-104.

Wotherspoon G, Lopez-Costa JJ, Michael GJ, Priestley JV (1997) Constitutive expression of calmodulin-binding phosphoprotein GAP-43 in rat serotonergic and noradrenergic cell groups which project to the spinal cord. Neurochem Res 22:985-993.

Zhang J, Madden TL (1997) PowerBLAST: new network BLAST application for interactive or automated sequence analysis and annotation. Genome Res 7:649–656.

Zhou LW, Moyer JA, Muth EA, Clark B, Palkovits M, Weiss B (1985) Regional distribution of calmodulin activity in rat brain. J Neurochem 44:1657-1662.

Zhou Q, Imbe H, Dubner R, Ren K (1999) Persistent Fos protein expression after orofacial deep or cutaneous tissue inflammation in rats: implications for persistent orofacial pain. J comp Neurol 412:276-291.

Ziegenhagen R, Gehrke P, Jennissen HP (1988) Covalent conjugation of mammalian calmodulin with ubiquitin. FEBS Lett 237:103-107.

Ziegenhagen R, Goldberg M, Rakutt WD, Jennissen HP (1990) Multiple ubiquitination of calmodulin results in one polyubiquitin chain linked to calmodulin. FEBS Lett 271:71-75.

**Publications directly related to the thesis:**

Bakota L., Orojan I., Gulya K. (2005) Intranuclear differences in calmodulin gene expression in the trigeminal nuclei of the rat. *Acta Biol. Szeged.* 49, 9-14.

Orojan I., Bakota L., Gulya K. (2006) Differential calmodulin gene expression in the nuclei of the rat midbrain-brain stem region. *Acta Histochemica* 108, 455-462.

Orojan I., Szigeti C., Varszegi S., Gulya K. (2006) Dithranol abolishes UCH-L1 immunoreactivity in the nerve fibers of the rat orofacial skin. *Brain Research* 1121, 216-220.

Orojan I., Bakota L., Szigeti C., Varszegi S., Gulya K. (2008) Experimentally induced orofacial inflammation and subsequent orticosteroid treatment differentially regulate calmodulin gene expression in the trigeminal nuclei of the rat. *Neurochem. Internat.* 52: 265-271.

**Presentations (talks, posters) directly related to the thesis:**

Orojan I., Bakota, L., Szigeti C., Varszegi S., Gulya K. (2005) Orofacial skin inflammation upregulates calmodulin gene expression in the trigeminal nuclei of the rat. 3rd International Workshop for the Study of Itch, Heidelberg (poster No. 8) *Acta Derm. Venereol.* 85:477.

Orojan I., Bakota, L., Gulya K. (2005) Experimentally induced orofacial skin inflammation upregulates calmodulin (CaM) gene expression in the medullar nuclei of the rat. 14th Congress of the European Academy of Dermatology & Venereology, London (abstract reference No. 805) . *J. Eur. Acad. Dermatol. Venereol*. 19(2) P04.67.

Orojan I., Bakota L., Szigeti C., Varszegi S., Gulya K. (2005) Az orofaciális bőr gyulladása serkenti a calmodulin génexpressziót a patkány nyúltvelői magvaiban. *Bőrgyógyászati és Venerológiai Szemle* 81(6):*258/59*

Oroján I. (2006) Dithranol által kiváltott orofaciális gyulladás befolyásolja a calmodulin génexpressziót a patkány nyúltvelői magvaiban. *Magyar Bőrgyógyászok*

*Nagygyűlése*, a Magyar Dermatológiai Társaság Fekete Zoltán Alapítványának nyertes előadása, Budapest.

**Publications not directly related to the thesis:**

Oroján I., Török L. (1996) Mucocutan nyirokcsomó szindroma (Kawasaki szindroma). *Bőrgyógyászati és Venerológiai Szemle* 72:69-73.

Oroján I., Török L. (1997) Mucocutaneous lymph node syndrome (Kawasaki syndrome). *Acta Dermatovenerologica Alpina, Pannonica et Adriatica* 6:31-34.

Hajdú K., Török L., Oroján I. (1999) Bleomycin okozta flagellaris dermatitis. *Bőrgyógyászati és Venerológiai Szemle* 75:17-19.

**Presentations (talks, posters) not directly related to the thesis:**

Oroján I: Kawasaki szindroma. Fiatal Bőrgyógyászok Fóruma, Kecskemét, 1995

Oroján I.: Hepatitis C és a Porphiria Cutanea Tarda együttes előfordulása. Fiatal Bőrgyógyászok Fóruma, Kecskemét, 1996

Oroján I., Raffai S.: Pikkelysömörös betegek TLO 1 kezelésével szerzett első tapasztalataink. Fiatal Bőrgyógyászok Fóruma, Kecskemét, 1997

Oroján I.: Flagellaris dermatitis, Fiatal Bőrgyógyászok Fóruma, Kecskemét, 1998

Oroján I., Kirchner Á.: Röntgensugárzás indukálta scleroderma circumscriptum. Magyar Bőrgyógyászok Nagygyűlése, Budapest, 1998

Hajdú K., Török L., Oroján, I.: Flagellaartige Hyperpigmentierung durch Bleomycin. Tagung der Deutsch-Ungarischen Dermatologischen Gesselschaft gemeinsam mit dem Berufsverband der Deutschen Dermatologen e.V., Kassel, 1998

Oroján I.: Androgenetikus bőrtünetek kezelésének lehetőségei a bőrgyógyászati gyakorlatban. Magyar Nőorvos Társaság I. Endokrinológiai kongresszusa, Kecskemét, 2002

Oroján I.: Androgenetikus bőrtünetek kezelésének lehetőségei a bőrgyógyászati gyakorlatban. Magyar Nőorvos Társaság, Családvédő Kongresszus, Budapest, 2003

Oroján I.: Androgenetikus bőrtünetek kezelésének lehetőségei a bőrgyógyászati gyakorlatban. Magyar Nőorvos Társaság Déldunántúli Szekció Ülése, Zalakaros, 2003

Oroján I.: Androgenetikus bőrtünetek kezelésének lehetőségei a bőrgyógyászati gyakorlatban. Magyar Nőorvos Társaság Északmagyarországi Szekció Ülése, Székesfehérvár, 2003